

Article

IL-13R α 2 Regulates the IL-13/IFN- γ Balance during Innate Lymphoid Cell and Dendritic Cell Responses to Pox Viral Vector-Based Vaccination

Zheyi Li ¹ , Sreeja Roy ^{1,2} and Charani Ranasinghe ^{1,*}

¹ Molecular Mucosal Vaccine Immunology Group, Department of Immunology and infectious Disease, The John Curtin School of Medical Research, The Australian National University, Canberra, ACT 2601, Australia; zheyi.li@anu.edu.au (Z.L.); roys3@amc.edu (S.R.)

² Department of Immunology & Microbial Disease, Albany Medical College, 47 New Scotland Ave, Albany, NY 12208-3479, USA

* Correspondence: Charani.ranasinghe@anu.edu.au; Tel.: +61-2-6125-4706

Abstract: We have shown that manipulation of IL-13 and STAT6 signaling at the vaccination site can lead to different innate lymphoid cell (ILC)/dendritic cell (DC) recruitment, resulting in high avidity/poly-functional T cells and effective antibody differentiation. Here we show that permanent versus transient blockage of IL-13 and STAT6 at the vaccination site can lead to unique ILC-derived IL-13 and IFN- γ profiles, and differential IL-13R α 2, type I and II IL-4 receptor regulation on ILC. Specifically, STAT6^{-/-} BALB/c mice given fowl pox virus (FPV) expressing HIV antigens induced elevated ST2/IL-33R⁺ ILC2-derived IL-13 and reduced NKp46^{+/-} ILC1/ILC3-derived IFN- γ expression, whilst the opposite (reduced IL-13 and elevated IFN- γ expression) was observed during transient inhibition of STAT6 signaling in wild type BALB/c mice given FPV-HIV-IL-4R antagonist vaccination. Interestingly, disruption/inhibition of STAT6 signaling considerably impacted IL-13R α 2 expression by ST2/IL-33R⁺ ILC2 and NKp46⁻ ILC1/ILC3, unlike direct IL-13 inhibition. Consistently with our previous findings, this further indicated that inhibition of STAT6 most likely promoted IL-13 regulation via IL-13R α 2. Moreover, the elevated ST2/IL-33R⁺ IL-13R α 2⁺ lung ILC2, 24 h post FPV-HIV-IL-4R antagonist vaccination was also suggestive of an autocrine regulation of ILC2-derived IL-13 and IL-13R α 2, under certain conditions. Knowing that IL-13 can modulate IFN- γ expression, the elevated expression of IFN- γ R on lung ST2/IL-33R⁺ ILC2 provoked the notion that there could also be inter-regulation of lung ILC2-derived IL-13 and NKp46⁻ ILC1/ILC3-derived IFN- γ via their respective receptors (IFN- γ R and IL-13R α 2) at the lung mucosae early stages of vaccination. Intriguingly, under different IL-13 conditions differential regulation of IL-13/IL-13R α 2 on lung DC was also observed. Collectively these findings further substantiated that IL-13 is the master regulator of, not only DC, but also different ILC subsets at early stages of viral vector vaccination, and responsible for shaping the downstream adaptive immune outcomes. Thus, thoughtful selection of vaccine strategies/adjuvants that can manipulate IL-13R α 2, and STAT6 signaling at the ILC/DC level may prove useful in designing more efficacious vaccines against different/chronic pathogens.

Keywords: ILC; DC; IL-4R antagonist and IL-13R α 2 adjuvants; STAT6; IL-13; IL-4/IL-13 receptor regulation; viral vector vaccination



Citation: Li, Z.; Roy, S.; Ranasinghe, C. IL-13R α 2 Regulates the IL-13/IFN- γ Balance during Innate Lymphoid Cell and Dendritic Cell Responses to Pox Viral Vector-Based Vaccination. *Vaccines* **2021**, *9*, 440. <https://doi.org/10.3390/vaccines9050440>

Academic Editor: Randy A. Albrecht

Received: 5 March 2021

Accepted: 23 April 2021

Published: 1 May 2021

Publisher's Note: MDPI stays neutral with regard to jurisdictional claims in published maps and institutional affiliations.



Copyright: © 2021 by the authors. Licensee MDPI, Basel, Switzerland. This article is an open access article distributed under the terms and conditions of the Creative Commons Attribution (CC BY) license (<https://creativecommons.org/licenses/by/4.0/>).

1. Introduction

Cytokines IL-13 and IL-4 have been well studied in models that are related to Th2 immunity, such as allergy, asthma, parasitic, and helminth infections [1–5]. The roles of these two cytokines have been characterized as the regulators of Th1 and Th2 immune responses [4–6]. IL-4 and IL-13 signal via a common receptor system [7], where the type I and type II IL-4 receptor complexes consist of the γ C/IL-4R α and IL-4R α /IL-13R α 1, respectively [8]. IL-4 binds to the type I receptor complex IL-4R α with high affinity,

and type II receptor complex with low affinity [9,10], activating the JAK/STAT6 pathway [11,12]. IL-13 can also bind to IL-13R α 1 of the type II IL-4 receptor complex, with low affinity (nM concentrations) and initiate signaling via the JAK/STAT6 pathway [8]. Furthermore, under low IL-13 conditions (pM concentrations), IL-13 is also thought to signal via the not well-characterized IL-13R α 2 pathway [13], involving STAT3 and activation of TGF- β 1 [14]. Several studies have now shown that IL-13R α 2 can bind to IL-4R α cytoplasmic tail and inhibit IL-4/IL-13 signaling via the IL-13R α 1/IL-4R α type II complex and JAK/STAT6 [15–18]. Moreover, in cancer studies, IL-13R α 2 activation/signaling has been associated with TGF- β production in the absence of functional IL-4R α [19]. Interestingly, dysregulation of IL-13R α 2 has been associated with many cancers [20–23].

The ILC are lineage negative cytokine-producing cells, which neither express lymphoid differentiation lineage markers nor T or B cell receptors. ILCs are generally divided into three distinct subsets, ILC1, ILC2, and ILC3, based on expression of cytokines, phenotypic markers, and transcription factors. Specifically, ILC2 are characterized by tissue specific surface expression of ST2/IL-33R (lung), IL-25R (muscle), or thymic stromal lymphopoietin receptor (TSLPR) (skin), and cytokines IL-4, IL-5, and IL-13, plus transcription factor GATA3 [24–27]. ILC1 and ILC3 are defined by the expression of NKp46, and their IFN- γ , IL-22, and IL-17A production capacity and linked to transcription factors T-bet and ROR γ t [27]. However, several studies have shown that the ILC populations can be highly plastic according to different cell/tissue milieus [24,25,28,29]. Recent studies in our laboratory have shown that following viral vector-based vaccination, ILC2 was the major source of IL-13 at the vaccination site 24 h post-delivery [24,30]. This was also linked to differential DC recruitment and downstream adaptive immune outcomes, which were also route dependent [24,31–36], suggesting that the optimal balance/regulation of IL-13 at the first line of defense was likely crucial for cell homeostasis and immune regulation.

Recently, we have designed two poxviral vector-based HIV vaccines that transiently manipulate IL-13 and IL-4 activity at the vaccination site to improve vaccine efficacy [32,33]. The IL-13R α 2 adjuvanted vaccine co-expressed HIV antigens together with soluble IL-13R α 2, which transiently sequestered IL-13 at the vaccination site [24,32]. The IL-4R antagonist adjuvanted vaccine co-expressed HIV antigens together with C-terminal deletion mutant of the mouse IL-4, lacking the essential tyrosine required for signaling. This antagonist was able to bind to both type I and type II IL-4 receptor complexes and transiently block both IL-4 and IL-13 signaling via the STAT6 pathway [33]. In a prime-boost modality, these vaccines were able to induce high avidity/poly-functional HIV specific mucosal and systemic CD4/CD8 T cells with improved protective efficacy, both in mice and macaques [31–35]. Moreover, in the context of humoral immunity, the IL-4R antagonist adjuvant vaccine was able to induce effective HIV gag-specific IgG1 and IgG2a differentiation in mice, unlike IL-13R α 2 adjuvanted vaccine [33]. To further confirm the role of IL-13 in antibody differentiation, when a cohort of knockout mice were vaccinated with unadjuvanted prime-boost strategy, although IL-4 $^{-/-}$ and STAT6 $^{-/-}$ animals showed enhanced IgG2a, IL-13 $^{-/-}$ mice showed extremely low IgG2a antibody responses [37]. More interestingly, when STAT6 $^{-/-}$ mice were given the IL-13R α 2 adjuvanted vaccine, elevated IgG1 and low IgG2a antibody responses were observed, similarly to the IL-13 $^{-/-}$ mice given the unadjuvanted vaccine [37]. These observations clearly indicated that the presence of IL-13 at the vaccination site was critical for effective antibody differentiation, and an STAT6 independent pathway was involved in this process, likely associated with IL-13R α 2 [37]. Interestingly, IFN- γ is also known to play an important role in antibody differentiation [38–42]. Moreover, during inflammation, IFN- γ has shown to inhibit ILC2 activation and IL-5 production [43], and similarly, under airway hyperreaction and asthma conditions IFN- γ has also shown to directly inhibit ILC2 function [44,45]. Recently we have also shown an interesting association of IL-13R α 2 and IFN- γ R with different DC subsets under different IL-13 conditions [14]. However, the relationship between IL-13 and IFN- γ at the ILC/DC level in the context of viral vector-based vaccination, and the

molecular mechanism by which ILC2-derived IL-13 regulates ILC1/ILC3 or DC activity, remain elusive.

Therefore, in this study wild type (WT) BALB/c, IL-13, and STAT6 gene knockout mice on BALB/C background were vaccinated with unadjuvanted (FPV-HIV) and WT BALB/c mice with IL-13R α 2 or IL-4R antagonist adjuvanted viral vector-based vaccines (two models which cause enduring and transient inhibition of IL-4/IL-13/STAT6, respectively), to unravel the IL-4/IL-13 receptor regulation mechanisms on ILC and DC under different IL-13 conditions.

2. Materials and Methods

Mice: 5–6 week old female wild type (WT) BALB/c, IL-13 $^{-/-}$, and STAT6 $^{-/-}$ mice on BALB/c background were obtained from the Australian Phenomics Facility, the Australian National University.

Ethics Statement: All animals were maintained and experiments performed in accordance with the Australian National Health and Medical Research Council (NHMRC) guidelines, within the Australian Code of Practice for the Care and Use of Animals for Scientific Purposes. The animal ethics were approved by The Australian National University's Animal Experimentation and Ethics Committee (AEEC). Protocol numbers A2014/14, and A2017/15.

Immunization: ILC studies, WT BALB/c mice were immunized with unadjuvanted FPV-HIV vaccine as control. IL-13 $^{-/-}$ and STAT6 $^{-/-}$ mice were also given the unadjuvanted FPV-HIV vaccine (which represented permanent IL-13 and STAT6 inhibition conditions, respectively) [36]. Another set of WT BALB/c mice were also immunized with FPV-HIV-IL-13R α 2 or FPV-HIV-IL-4R antagonist adjuvanted vaccines (which represented transient inhibition of IL-13 or IL-4/IL-13 signaling via STAT6, respectively) [7,32–35,46,47]. DC studies, FPV-HIV (rFPV) or VV-HIV (rVV) were administered to WT BALB/c mice. Each vaccine 10⁷ PFU was administered intranasally (i.n.) to mice (n = 4 to 6) under mild isoflurane anesthesia. Vaccines were diluted in sterile PBS, sonicated 3 times (15 s each time) on ice at 50 outputs using a Branson Sonifier 450 prior to administration, and given 10–15 μ L per nostril (total 25–30 μ L volume). Note that: (i) all vaccines were prepared as described previously [32,33,48]; (ii) rFPV is a non-replicating vector, and all co-expressed antigens/adjuvants were expressed for less than 72 h (transiently), which was also established by imaging studies [49,50], unlike rVV, which is a replicating vector that can express for much longer periods.

Preparation of lung lymphocytes: The mice were euthanized using cervical dislocation according to the approved AEEC guidelines. Lung tissues were removed and kept in complete RPMI medium (Sigma) on ice until processing. Single cell lung suspensions were prepared as described previously [24,32]. Specifically, the lung tissues were first cut into small pieces, and then enzymatically digested in 1 mL of digestion buffer containing 1 mg/mL collagenase (Sigma-Aldrich, St Louis, MO, USA), 1.2 mg/mL Dispase (Gibco, Auckland, New Zealand), and 5 Units/mL DNase (Calbiochem, La Jolla, CA, USA) in complete RPMI. During digestion, samples were gently vortexed every 10 min and incubated in a 37 °C water bath for 45 min. The digested lung tissues were mashed and passed through a 100 μ m Falcon cell strainer and the resulting lung cell suspensions were centrifuged for 15 min at 1500 RPM (524 \times g) at 4 °C using a Beckman ALLEGRA X-12R centrifuge. Next, the supernatants were removed, cells were resuspended in 5 mL red blood cell lysis buffer (at room temperature) containing 0.16 mM NH₄Cl and 0.17 M Tris HCl (pH 7.65) for 3 min at room temperature, 30 mL of complete RPMI medium was added, and centrifuged at 1500 RPM (524 \times g) for 5 min at 4 °C. Cells were washed once more with complete RPMI and passed through sterile gauze to remove any remaining debris, followed by two washes in complete RPMI medium, and the cell pellets were then resuspended in 0.5 mL complete RPMI medium, counted using a hemocytometer (Tiefe Depth Profondeur 0.100 mm), and stored on ice until use.

Flow cytometry staining of ILC subsets and IL-4/IL-13 receptors: 2×10^6 cells per sample were plated into U-bottomed 96-well plates (Falcon) and rested for 16 h at 37 °C with 5% CO₂ in a Forma Scientific water-jacketed incubator, to allow the recovery of cell surface markers before performing the surface and intracellular staining [32]. Prior to staining, $1 \times$ Brefeldin A (BFA) was added to each sample and incubated at 37 °C with 5% CO₂ for 5 h to prevent cytokine release. Surface and intracellular staining were performed as described previously [24]. Basically, cells were washed twice with FACS buffer (2% FCS in PBS), and FC block antibody (PharMingen clone 2.4G2) was added to reduce non-specific binding. Then cells were washed, and surface staining was performed for 40 min with the respective antibodies, including the IL-4/IL-13 receptors. Cells were next washed, fixed with IC-FIX buffer (Biolegend, San Diego, CA, USA), and permeabilized using IC-PERM buffer (Biolegend). Intracellular antibodies were then added for 30 min, washed, and cells were fixed with 0.5% PFA. Specifically, ILC2 staining; APC/Cy7-conjugated anti-mouse CD45 (Biolegend clone 30-F11) and FITC-conjugated lineage cocktail (CD3 (Biolegend clone 17A2), CD19 (Biolegend clone 6D5), CD11b (Biolegend clone M1/70), CD11c (Biolegend clone N418), CD49b (Biolegend clone HM α 2), Fc ϵ RI (Biolegend clone MAR1)) were used to gate out the lineage-cells. PE-conjugated or PerCP/Cy5.5-conjugated anti-mouse ST2/IL-33R (Biolegend clone DIH9) was used to identify the lung ILC2. PE-eFlour 610-conjugated anti-mouse IL-13 (eBioscience clone EBio13A) was used to evaluate intracellular expression of IL-13 in ILC2s. For ILC1/ILC3 staining; APC/Cy7-conjugated anti-mouse CD45 (Biolegend clone 30-F11), and the same FITC-conjugated lineage cocktail were used to identify lineage-cells. PE-conjugated or PerCP/Cy5.5-conjugated anti-mouse ST2/IL-33R (Biolegend clone DIH9), and Brilliant Violet 421-conjugated anti-mouse CD335 (NKp46) (Biolegend clone 29A1.4) were used to identify ILC1/3 populations. Brilliant Violet 510-conjugated anti-mouse IFN- γ (Biolegend XMG1.2) was used to evaluate intracellular expression of IFN- γ in ILC1 and ILC3 and intracellular staining was performed as for ILC2.

PE-conjugated anti-mouse γ C (CD132) (PharMingen clone 554457), PE-conjugated anti-mouse IL-4R α (CD124) (Biolegend clone I015F8), PE-conjugated anti-mouse IL-13R α 1 (eBioscience clone 13MOKA), and Biotin-conjugated anti-mouse IL-13R α 2 (R&D, clone BAF539) were used to evaluate type I (γ C and IL-4R α) and type II (IL-4R α and IL-13R α 1) IL-4 receptor complex and IL-13R α 2 expression on different ILC subsets. PE-conjugated streptavidin (Biolegend) was used as a secondary antibody to detect the Biotin-conjugated IL-13R α 2 antibody. All receptor antibodies were stained separately, to avoid spectral overlap. Specifically, γ C (PE), IL-4R α (PE), IL-13R α 1 (PE), and IL-13R α 2 (Biotin) were stained with ILC master mix antibodies. Then γ C, IL-4R α , and IL-13R α 1-stained samples were directly fixed with 0.5% PFA. The IL-13R α 2-stained samples were washed once with FACS buffer and then stained with PE-conjugated Streptavidin for 15 min on ice in the dark, followed by washing and fixing with 0.5% PFA. A total of 1,000,000 events were acquired per sample and analyzed using a BD LSR Fortessa. All ILC subsets and their γ C, IL-4R α , IL-13R α 1, and IL-13R α 2 expression were analyzed based on the fluorescent minus one (FMO) control, as described in Figure S1.

Evaluation of IL-4 and IL-13 receptor expression on lung cDCs and pDCs using flow cytometry: Lung tissues were harvested and prepared into single cell suspensions as for the ILC studies, 24, 48, or 72 h post vaccination. Then, 2×10^6 cells from each sample were blocked with anti-mouse CD16/CD32 Fc Block antibody (BD Biosciences, San Jose, CA, USA) for 20 min at 4 °C, and cells were stained with DC markers, APC-conjugated anti-mouse MHCII I-Ad (e-Biosciences, San Diego, CA, USA), biotin-conjugated anti-mouse CD11c (N418 clone, Biolegend, San Diego, CA, USA), followed by streptavidin Brilliant violet 421 (Biolegend, San Diego, CA, USA), anti-mouse CD11b AlexaFluor 700 (M1170 clone, Biolegend, San Diego, CA, USA), anti-mouse CD103 FITC (2E7 clone, eBiosciences, San Diego, CA, USA), and anti-mouse B220 PercpCy5.5 (RA3-6B2 clone, e-Biosciences, San Diego, CA, USA) for 30 min on ice. To evaluate IL-4 and IL-13 receptors, cells were also extracellularly stained with either anti-mouse IL-4R α (CD124) PE (I015F8 clone, Biolegend, San Diego, CA, USA), anti-mouse IL-13R α 1 (CD213a) PE (13MOKA clone, eBiosciences,

San Diego, CA, USA), or Biotin-conjugated anti-mouse IL-13R α 2 (110815 clone, R&D systems, Minneapolis, MN, USA), followed by streptavidin PE (Biolegend, San Diego, CA, USA), anti-mouse γ C (CD132) PE (TUGm2 clone, Biolegend, San Diego, CA, USA). Cells were fixed using 1.5% paraformaldehyde, resuspended in PBS and analyzed using a BD LSRII flow cytometer (Becton Dickinson, San Diego, CA, USA). A total of 5×10^5 events per sample were acquired and the results were analyzed using FlowJo software v10.0.7 and the gating strategies described in Figure S7.

Statistical analysis: In this study, cell numbers were calculated using the formula (number of receptor or cytokine expressing cells/number of CD45⁺ cells) $\times 10^6$. Results are represented as a percentage of CD45⁺ cells, and can also be found in the supplementary figures (Figure S7). IL-4 and IL-13 receptor proportions on lung DCs were calculated as a percentage of parent MHC-II⁺ CD11c⁺ CD11b⁺ CD103⁻ cDC and MHC-II⁺ CD11c⁺ CD11b⁻ B220⁺ pDC population. Note that less than 10 cells expressing the receptor was set as a cut-off. Statistical analysis was performed using GraphPad Prism software (version 6.05 for Windows). One-way ANOVA using Tukey's multiple comparisons test and unpaired *t*-test were used. The *p*-values are denoted as: ns—*p* \geq 0.05, *—*p* < 0.05, **—*p* < 0.01, ***—*p* < 0.001, ****—*p* < 0.0001. All experiments were repeated at least three times.

3. Results

3.1. Following rFPV Vaccination; ILC2-Derived IL-13 and ILC1/ILC3-Derived IFN- γ Expression Was Inversely Correlated

Mice were immunized with the unadjuvanted FPV-HIV, FPV-HIV-IL-4R antagonist, or FPV-HIV-IL-13R α 2 adjuvanted vaccines as described in the materials and methods. Then, 24 h post vaccination, IL-33R/ST2⁺ ILC2-derived IL-13 and NKp46^{+/−} ILC1/ILC3-derived IFN- γ expression profiles were evaluated using multicolor flow cytometry and gating strategy, indicated as described previously [24] (Figure S1). In this study the STAT6^{−/−} mice given the unadjuvanted vaccine showed the highest IL-33R/ST2⁺ ILC2-derived IL-13 expression and the lowest NKp46^{+/−} ILC1/ILC3-derived IFN- γ expression compared to all the other vaccine groups tested (Figure 1a–c). Interestingly, an inverse relationship was observed when WT BALB/c mice were given the FPV-HIV-IL-4R antagonist vaccination (Transient inhibition of STAT6 signaling) (Figure 1a–c). The IL-13^{−/−} mice given the unadjuvanted vaccine showed much greater IFN- γ expression by both NKp46^{+/−} ILC1/ILC3 compared to the WT BALB/c mice given the FPV-HIV-IL-13R α 2 adjuvanted vaccination (transient inhibition of IL-13) (*p* < 0.01) (Figure 1b,c). Between the different vaccination conditions tested the IL-33R/ST2⁺ ILC2-derived IL-13 expression profile was in the order: STAT6^{−/−} unadjuvanted > WT unadjuvanted > FPV-HIV-IL-4R antagonist or FPV-HIV-IL-13R α 2 adjuvanted > IL-13^{−/−} unadjuvanted vaccination. Whereas, the ILC1/ILC3-derived IFN- γ expression profile was WT unadjuvanted and FPV-HIV-IL-4R antagonist adjuvanted > IL-13^{−/−} unadjuvanted > FPV-HIV-IL-13R α 2 adjuvanted > STAT6^{−/−} unadjuvanted vaccination. No ILC2-derived IL-4 expression was detected in any of the vaccine groups tested. (For data presented in the form of percentage of CD45⁺ cells, please see Figure S7a).

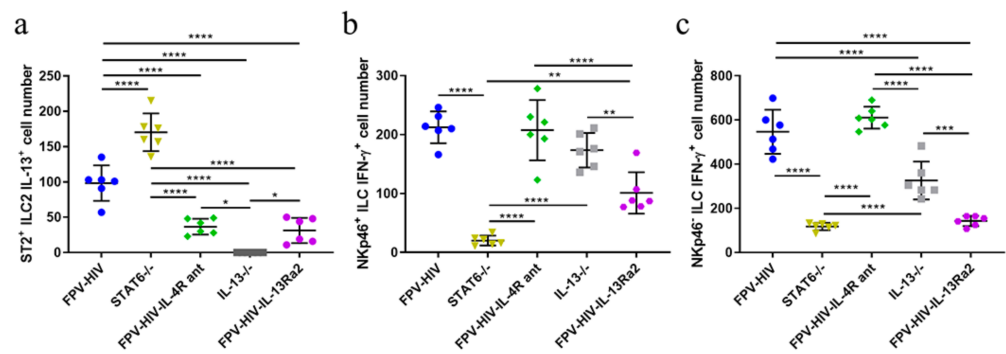


Figure 1. Comparison of ILC2-driven IL-13 and ILC1/ILC3-driven IFN- γ expression following rFPV vaccination under permanent (knock out mice) vs. transient inhibition of IL-13 and STAT6. Color coded vaccine groups represent: blue, WT BALB/c given FPV-HIV (control); yellow, STAT6^{-/-} given FPV-HIV (which represents permanent STAT6 signaling inhibition condition); green, WT BALB/c given FPV-HIV-IL-4R antagonist vaccine (which represents transient IL-4/IL-13/STAT6 signaling inhibition condition); grey, IL-13^{-/-} given FPV-HIV (which represents permanent IL-13 inhibition condition); and purple, WT BALB/c given FPV-HIV-IL-13 α 2 adjuvanted vaccine (which represents transient IL-13 sequestration/inhibition condition). Graphs represent IL-13 expression by lung IL-33R/ST2⁺ ILC2 (a) and IFN- γ expression by lung NKp46^{-/+} ILC1/ILC3 (b,c) following IL-13^{-/-} and STAT6^{-/-} BALB/c background mice (n = 4) given the control unadjuvanted vaccine (FPV-HIV) compared to BALB/c mice (n = 4) given FPV-HIV unadjuvanted, FPV-HIV-IL-4R antagonist, and FPV-HIV-IL-13R α 2 adjuvanted vaccines. The error bars represent the mean and standard deviation (s.d.). The p values were calculated using One-way ANOVA using Tukey's multiple comparisons test and unpaired t-test. * p < 0.05, ** p < 0.01, *** p < 0.001, **** p < 0.0001. Experiments were repeated a minimum 3 times. Note that in the figure FPV-HIV-IL-4R ant represents FPV-HIV-IL-4R antagonist.

3.2. Elevated Number of ST2/IL-33R⁺ ILC2 and NKp46⁻ ILC1/ILC3 Expressed IL-13R α 2 Following FPV-HIV-IL-4R Antagonist Vaccination, Unlike STAT6^{-/-} Given FPV-HIV

To examine type I and type II IL-4 receptor complexes and IL-13R α 2 expression profiles on different ILC subsets, STAT6^{-/-} and WT BALB/c mice were vaccinated intranasally with the unadjuvanted or adjuvanted rFPV vaccines. ILC profiles were evaluated 24 h post vaccination using the multicolor flow cytometry and gating strategy described in the materials and methods (Figures S1 and S2). Interestingly, vaccination under transient versus permanent STAT6 inhibition showed significantly different IL-13R α 2 and IL-4R α type I receptor (IL-4R α / γ C) expression profiles on lung ST2/IL-33R⁺ ILC2. Specifically, an elevated number of ST2/IL-33R⁺ ILC2 were found to express IL-13R α 2 following IL-4R antagonist adjuvanted vaccination compared to WT BALB/c mice given the unadjuvanted FPV-HIV vaccination (p < 0.05) (Figure 2a), whereas no expression of IL-13R α 2 was observed in ST2/IL-33R⁺ ILC2 obtained from STAT6^{-/-} mice given the unadjuvanted vaccine (Figure 2a). Moreover, although no differences in IL-4R α and γ C expression were detected in ST2/IL-33R⁺ ILC2 obtained from WT BALB/c mice vaccinated with IL-4R antagonist adjuvanted and unadjuvanted vaccines, STAT6^{-/-} mice given unadjuvanted FPV-HIV vaccine showed significantly lower expression of these two receptors (Figure 2c,d). Interestingly, IL-13R α 1 expression on ST2/IL-33R⁺ ILC2 was not significantly different in the three vaccination groups tested (Figure 2b).

Next, when the densities (mean fluorescence intensities) of these receptors were accessed, no significant differences in IL-13R α 2 and IL-13R α 1 were detected on ST2/IL-33R⁺ ILC2s (Figure S3). However, IL-4R α densities on ST2/IL-33R⁺ ILC2 obtained from STAT6^{-/-} mice given the unadjuvanted vaccine were significantly down-regulated compared to WT BALB/c mice given the adjuvanted or the unadjuvanted vaccines (p < 0.0001 and p < 0.001 respectively) (Figure S3c). Similarly, down regulation of γ C on ST2/IL-33R⁺ ILC2 was also observed in STAT6^{-/-} mice compared to WT BALB/c given the unadjuvanted vaccine (Figure S3d).

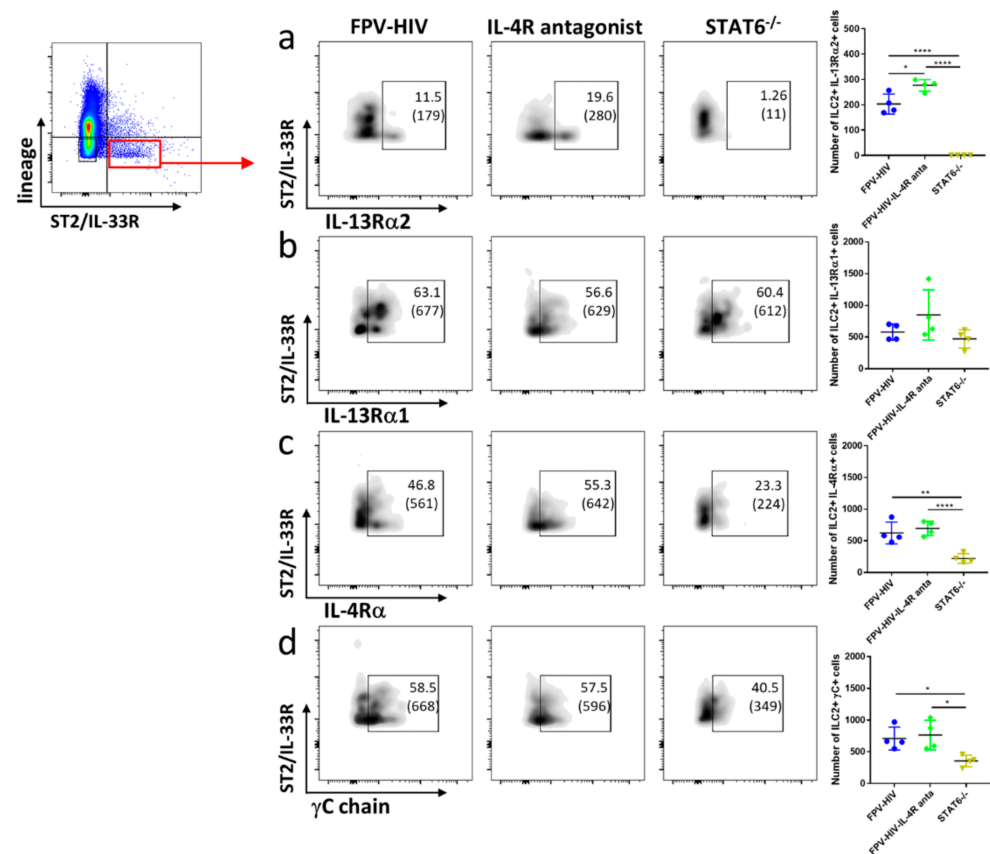


Figure 2. Evaluation of lung lineage⁻ IL-33R/ST2⁺ ILC2 expressing type I (γ C/IL-4R α), type II (IL-4R α /IL-13R α 1) IL-4 receptor complexes and IL-13R α 2 following vaccination under permanent vs. transient inhibition of STAT6. WT BALB/c and STAT6^{-/-} mice on BALB/c background (n = 4) were immunized intranasally with FPV-HIV-IL-4R antagonist adjuvanted or FPV-HIV unadjuvanted vaccines, respectively. Color coded vaccine groups represent: blue, WT BALB/c given FPV-HIV (control); green, WT BALB/c given FPV-HIV-IL-4R antagonist vaccine (which represents transient IL-4/IL-13/STAT6 signaling inhibition condition); and yellow, STAT6^{-/-} given FPV-HIV (which represents permanent STAT6 signaling inhibition condition). Lung ILC2s were identified as CD45⁺ FSC^{low} SSC^{low} lineage⁻ IL-33R/ST2⁺ cells. The FACS plots in each panel indicate the percentage of ILC2 expressing IL-13R α 2 (a), IL-13R α 1 (b), IL-4R α (c), and γ C chain (d) in each vaccinated group. The bracket below the cell percentage indicates the number of cells in each gate. The graph in each panel represents the number of ILC2s expressing the different receptors back calculated to CD45⁺ population as described in the materials and methods (24 h post vaccination). The error bars represent the mean and standard deviation (s.d.). The *p* values were calculated using one-way ANOVA using Tukey's multiple comparisons test and unpaired *t*-test. * *p* < 0.05, ** *p* < 0.01, **** *p* < 0.0001. Experiments were repeated a minimum of 3 times.

Similar to ST2/IL-33R⁺ ILC2, an elevated number of NKp46⁻ ILC1/ILC3 were found to express IL-13R α 2 in the FPV-HIV-IL-4R antagonist adjuvanted vaccine group compared to both WT BALB/c and STAT6^{-/-} mice given unadjuvanted FPV-HIV vaccination (*p* < 0.01) (Figure 3a). Interestingly, STAT6^{-/-} mice given unadjuvanted FPV-HIV vaccine showed down-regulation of the IL-13R α 1 on NKp46⁻ ILC1/ILC3 compared to WT BALB/c mice given the unadjuvanted FPV-HIV or FPV-HIV-IL-4R antagonist adjuvanted vaccines (Figure 3b). Moreover, transient inhibition of STAT6 signaling (WT BALB/c given FPV-HIV-IL-4R antagonist) down-regulated the expression of IL-4R α and γ C (type I IL-4 receptor complex) on NKp46⁻ ILC1/ILC3s (*p* < 0.05) (Figure 3c,d). In the context of IL-4/IL-13 receptor densities, STAT6^{-/-} mice given the unadjuvanted vaccine showed significant downregulation of IL-13R α 2 on NKp46⁻ ILC1/ILC3 compared to the other vaccine groups

tested (Figure S4a). Interestingly, IL-13R α 1 or IL-4R α was not modulated on NKp46 $^{-}$ ILC1/ILC3 under transient versus permanent blockage of STAT6 (Figure S4b,c), although STAT6 inhibition resulted in down-regulation of γ C expression (Figure S4d). (For data presented in the form of percentage of CD45 $^{+}$ cells, please see Figure S7b,c).

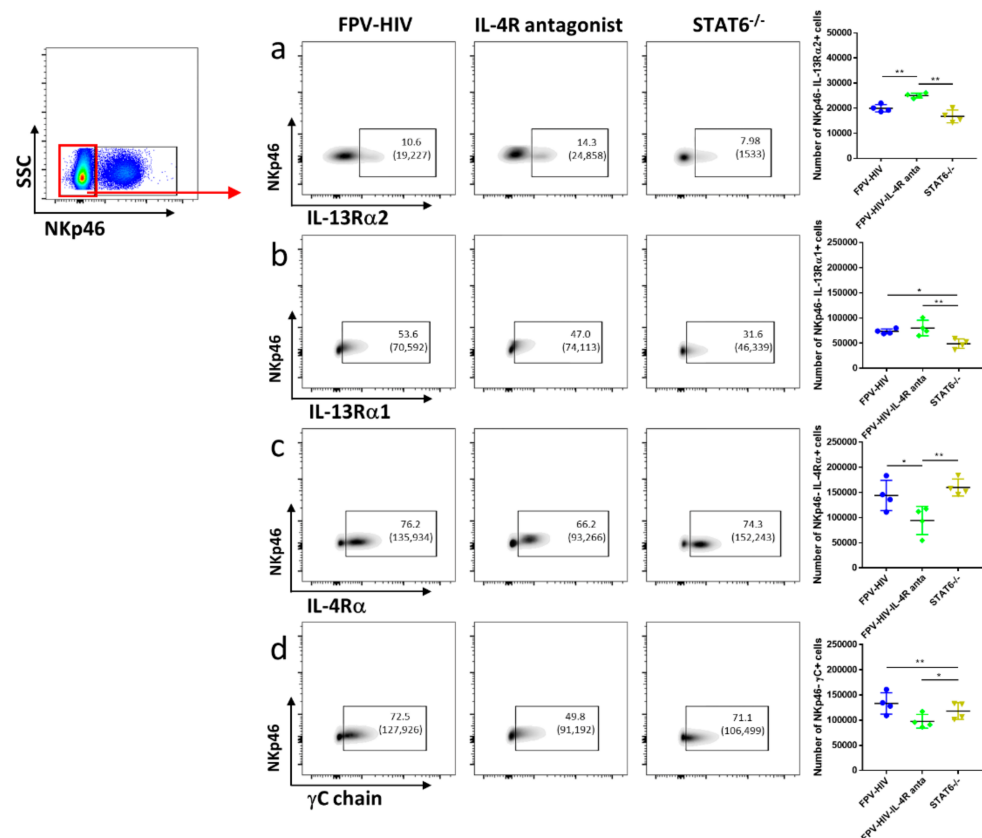


Figure 3. Evaluation of lung lineage $^{-}$ IL-33R/ST2 $^{-}$ NKp46 $^{-}$ ILC1/ILC3 expressing IL-13R α 2, IL-13R α 1, IL-4R α , and γ C following vaccination under permanent vs. transient inhibition of STAT6. WT BALB/c and STAT6 $^{-/-}$ mice on BALB/c background (n = 4) were immunized intranasally with FPV-HIV-IL-4R antagonist adjuvanted or FPV-HIV unadjuvanted vaccines, respectively. Color coded vaccine groups represent: blue, WT BALB/c given FPV-HIV (control); green, WT BALB/c given FPV-HIV-IL-4R antagonist vaccine (which represents transient IL-4/IL-13/STAT6 signaling inhibition condition); and yellow, STAT6 $^{-/-}$ given FPV-HIV (which represents permanent STAT6 signaling inhibition condition). Lung NKp46 $^{-}$ ILC1/ILC3 were gated as CD45 $^{+}$ FSC low SSC low lineage $^{-}$ IL-33R/ST2 $^{-}$ NKp46 $^{-}$ cells. The FACS plots in each panel indicate the percentage of NKp46 $^{-}$ ILC1/ILC3 expressing IL-13R α 2 (a), IL-13R α 1 (b), IL-4R α (c), and γ C chain (d). The bracket below the cell percentage indicates the number of cells in each gate. Graph in each panel represents the number of NKp46 $^{-}$ ILC1/ILC3s expressing the different receptors back calculated to CD45 $^{+}$ population, as described in the materials and methods at (24 h post vaccination). The error bars represent the mean and standard deviation (s.d.). The p values were calculated using one-way ANOVA using Tukey's multiple comparisons test and unpaired t-test. * p < 0.05, ** p < 0.01. Experiments were repeated a minimum of 3 times.

3.3. Following FPV-HIV-IL-13R α 2 Adjuvanted Vaccination, IL-13R α 2 Was Not Regulated on ST2/IL-33R $^{+}$ ILC2 or NKp46 $^{-}$ ILC1/ILC3, Unlike IL-13 $^{-/-}$ Given FPV-HIV Vaccination

Next, IL-4/IL-13 receptor expression on ST2/IL-33R $^{+}$ lung ILC2 was examined following vaccination under transient versus permanent IL-13 inhibition (WT BALB/C given FPV-HIV-IL-13R α 2 vs. IL-13 $^{-/-}$ given FPV-HIV). Although expression of IL-13R α 2 on ST2/IL-33R $^{+}$ ILC2 was not modulated, IL-13R α 1 expression was significantly down regulated in IL-13 $^{-/-}$ mice given the unadjuvanted vaccine (p < 0.05) (Figure 4a,b). Interestingly,

an elevated number of WT BALB/c ST2/IL-33R⁺ ILC2 were found to express both γ C and IL-4R α following FPV-HIV-IL-13R α 2 adjuvanted vaccination, unlike IL-13^{-/-} mice given unadjuvanted FPV-HIV vaccine ($p < 0.001$ and $p < 0.0001$, respectively) (Figure 4c,d). Furthermore, compare to the WT BALB/c mice given the unadjuvanted vaccine, WT mice that received the FPV-HIV-IL-13R α 2 adjuvanted vaccine showed significant regulation of type I IL-4 receptor complex (IL-4R α / γ C) on ST2/IL-33R⁺ ILC2 (Figure 4c,d). In the context of IL-4/IL-13 receptor densities, a significantly reduced IL-4R α / γ C expression was observed on IL-13^{-/-} ST2/IL-33R⁺ ILC2 given the unadjuvanted vaccine (Figure S5). Interestingly, IL-13R α 1 and IL-13R α 2 densities were not regulated in any of the vaccine groups tested (Figure S5).

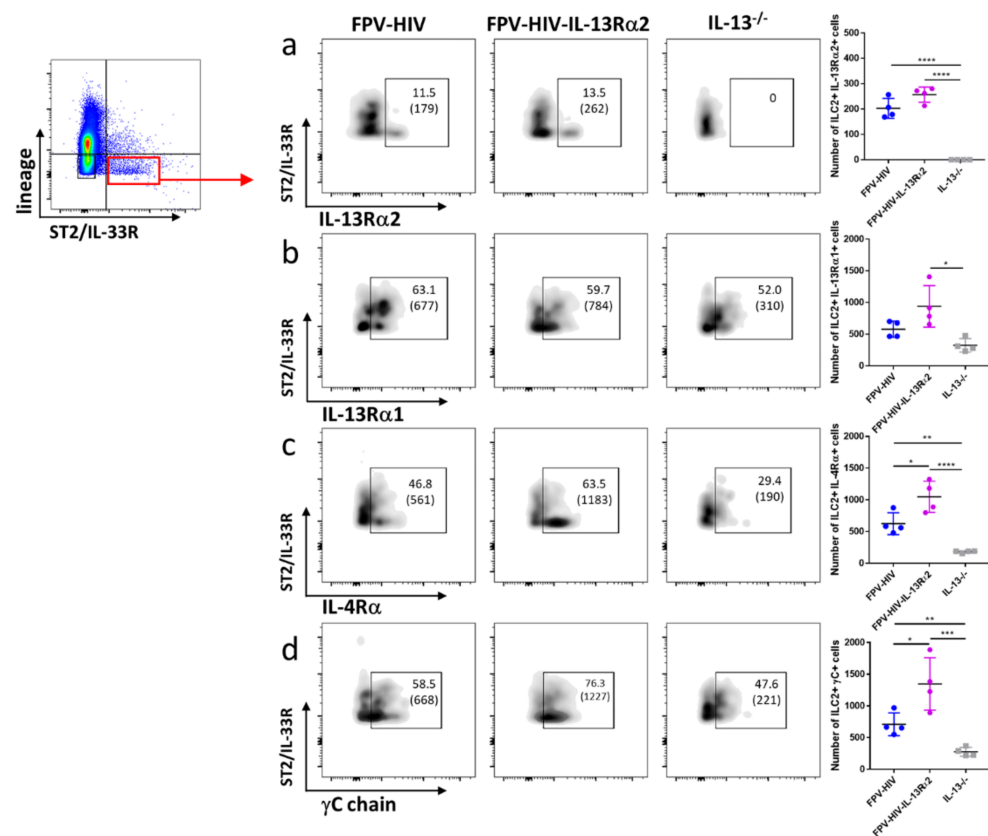


Figure 4. Evaluation of lung lineage⁻ IL-33R/ST2⁺ ILC2 expressing IL-13R α 2, IL-13R α 1, IL-4R α , and γ C following vaccination under permanent vs. transient inhibition of IL-13. WT BALB/c and IL-13^{-/-} mice on BALB/c background (n = 4) were immunized intranasally with FPV-HIV-IL-13R α 2 adjuvanted or FPV-HIV unadjuvanted vaccines. Color coded vaccine groups represent: blue, WT BALB/c given FPV-HIV (control); purple, WT BALB/c given FPV-HIV-IL-13 α 2 adjuvanted vaccine (which represents transient IL-13 sequestration/inhibition condition); and grey, IL-13^{-/-} given FPV-HIV (which represents permanent IL-13 inhibition condition). Lung ILC2 were gated as CD45⁺ FSC^{low} SSC^{low} lineage⁻ IL-33R/ST2⁺ cells. The FACS plots in each panel indicate the percentage of ILC2s expressing IL-13R α 2 (a), IL-13R α 1 (b), IL-4R α (c), and γ C chain (d). The bracket below the cell percentage indicates the number of cells in each gate. The graph in each panel represents the number of ILC2s expressing the different receptors back calculated to CD45⁺ population, as described in the materials and methods (24 h post vaccination). The error bars represent the mean and standard deviation (s.d.). The p values were calculated using one-way ANOVA using Tukey's multiple comparisons test and unpaired t -test. * $p < 0.05$, ** $p < 0.01$, *** $p < 0.001$, **** $p < 0.0001$. Experiments were repeated a minimum of 3 times.

Furthermore, a significantly elevated number of IL-13^{-/-} NKp46⁻ ILC1/ILC3s were found to express IL-13R α 2 given the unadjuvanted vaccine compared to WT BALB/c

mice given the unadjuvanted or adjuvanted vaccines ($p < 0.001$), where the latter two groups showed very similar IL-13R α 2 expression profiles (Figure 5a). However, surprisingly, transient inhibition of IL-13 showed an elevated number of NKp46 $^-$ ILC1/ILC3 expressing IL-13R α 1 compared to WT BALB/c and IL-13 $^{-/-}$ mice given the unadjuvanted vaccine ($p < 0.01$) (Figure 5b). In contrast, an elevated number of NKp46 $^-$ ILC1/ILC3s obtained from IL-13 $^{-/-}$ given the unadjuvanted vaccines were also found to express IL-4R α ($p < 0.05$) (Figure 5c), but not γ C (Figure 5d). In the transient versus permanent IL-13 inhibitory vaccination conditions, IL-13R α 2, IL-4R α , and γ C, but not IL-13R α 1 densities, were differentially regulated on NKp46 $^-$ ILC1/ILC3 (Figure S6). (For data presented in the form of percentage of CD45 $^+$ cells, please see Figure S7d,e).

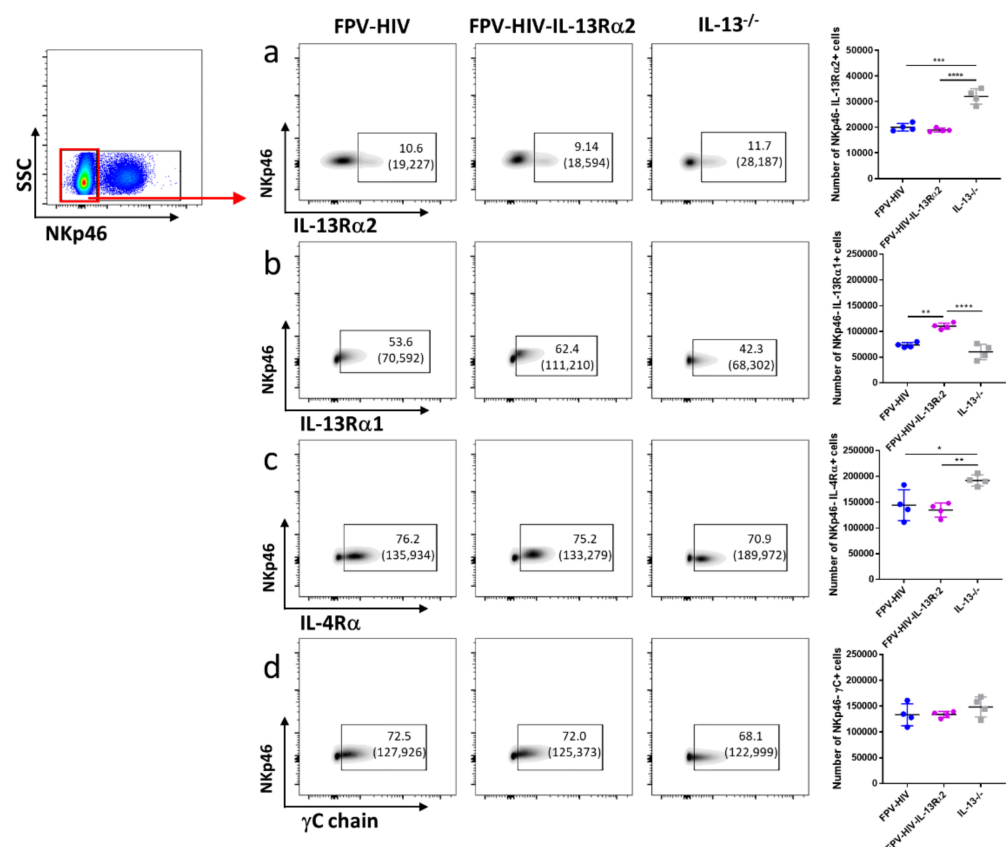


Figure 5. Evaluation of lung lineage $^-$ IL-33R/ST2 $^-$ NKp46 $^-$ ILC1/ILC3 expressing IL-13R2, IL-13R α 1, IL-4R α , and α C following vaccination under permanent vs. transient inhibition of IL-13. WT BALB/c and IL-13 $^{-/-}$ mice on BALB/c background (each group $n = 4$) were immunized intranasally with FPV-HIV-IL-13R α 2 adjuvanted or FPV-HIV unadjuvanted vaccines. Color coded vaccine groups represent: blue, WT BALB/c given FPV-HIV (control); purple, WT BALB/c given FPV-HIV-IL-13 α 2 adjuvanted vaccine (which represents transient IL-13 sequestration/inhibition condition); and grey, IL-13 $^{-/-}$ given FPV-HIV (which represents permanent IL-13 inhibition condition). Lung NKp46 $^-$ ILC1/ILC3 were gated as CD45 $^+$ FSC $^{\text{low}}$ SSC $^{\text{low}}$ lineage $^-$ IL-33R/ST2 $^-$ NKp46 $^-$ cells. The FACS plots in each panel indicate the percentage of NKp46 $^-$ ILC1/ILC3 expressing IL-13R α 2 (a), IL-13R α 1 (b), IL-4R α (c), and α C chain (d). The bracket below the cell percentage indicates the number of cells in each gate. The graph in each panel represents the number of NKp46 $^-$ ILC1/ILC3 expressing the different receptors 24 h post vaccination back calculated to CD45 $^+$ population, as described in the materials and methods. The error bars represent the mean and standard deviation (s.d.). The p values were calculated using one-way ANOVA using Tukey's multiple comparisons test and unpaired t -test. * $p < 0.05$, ** $p < 0.01$, *** $p < 0.001$, **** $p < 0.0001$. Experiments were repeated a minimum of 3 times.

3.4. Vaccination under Transient or Permanent Inhibition of IL-13 or STAT6 Signaling Did Not Modulate IL-13R α 2 Expression on NKp46 $^{+}$ ILC1/ILC3, Unlike NKp46 $^{-}$ ILC1/ILC3

When IL-4/IL-13 receptors on NKp46 $^{+}$ ILC1/ILC3 were accessed under transient versus permanent inhibition of IL-13 or STAT6 signaling, surprisingly there were no major differences in the number of NKp46 $^{+}$ ILC1/ILC3 expressing IL-13R α 2 (even though the number of cells expressing the receptor was lower in the KO mice compared to the BALB/c given the unadjuvanted vaccine, $p < 0.5$) (Figure 6a). In contrast, the number of NKp46 $^{+}$ ILC1/ILC3 expressing γ C, IL-4R α , and IL-13R α 1 (Figure 6b,c) was found to be significantly lower under permanent STAT6 or IL-13 inhibition (KO mice) compared to transient inhibition. Interestingly, both transient blockage of STAT6 (FPV-HIV-IL-4R antagonist vaccination of wild type mice) and IL-13 (FPV-HIV-IL-13R α 2 vaccination of wild type mice) showed a significantly elevated number of NKp46 $^{+}$ ILC1/ILC3 expressing γ C, IL-4R α , and IL-13R α 1 compared to BALB/c mice given the unadjuvanted FPV-HIV vaccine (Figure 6b,c). (For data presented in the form of percentage of CD45 $^{+}$ cells, please see Figure S7f).

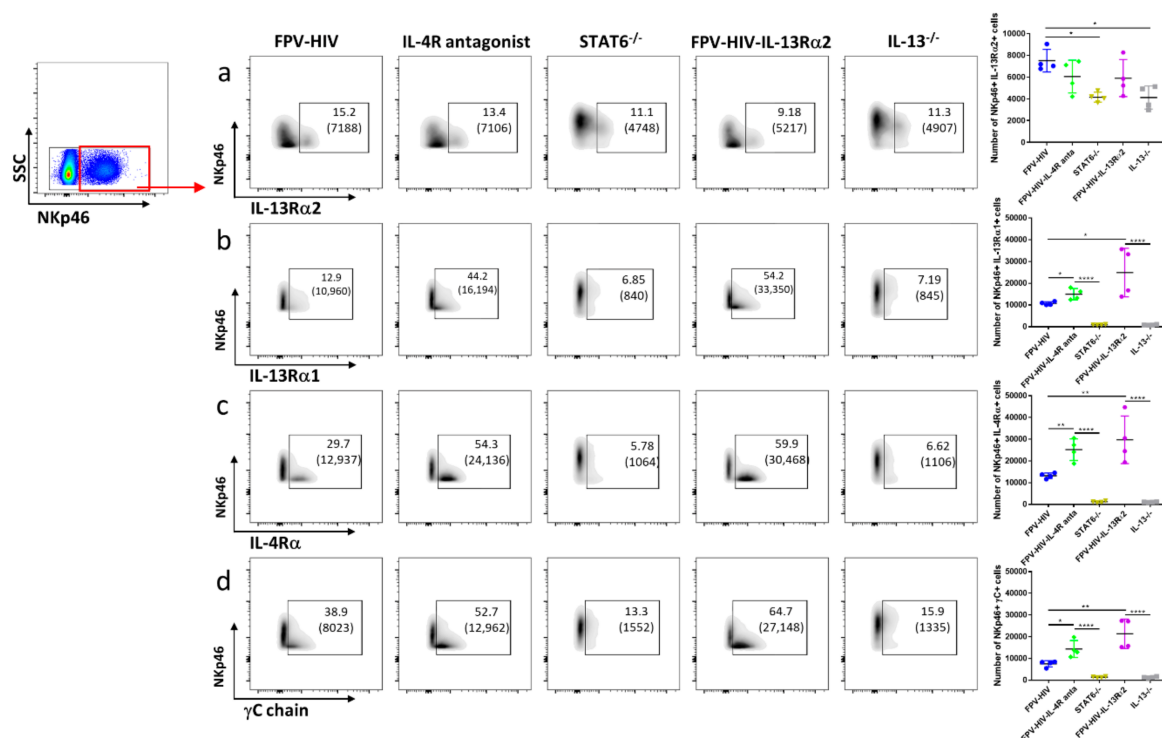


Figure 6. Evaluation of lung lineage $^{-}$ IL-33R/ST2 $^{-}$ NKp46 $^{+}$ ILC1/ILC3 expressing IL-13R α 2, IL-13R α 1, IL-4R α , and γ C receptors following rFPV vaccination under different inhibitory conditions. WT BALB/c mice ($n = 4$) were immunized intranasally with FPV-HIV-IL-4R antagonist or FPV-HIV-IL-13R α 2 adjuvanted vaccines. STAT6 $^{-/-}$ and IL-13 $^{-/-}$ mice on BALB/c background ($n = 4$) were immunized with FPV-HIV unadjuvanted vaccine. Color coded vaccine groups represent: blue, WT BALB/c given FPV-HIV (control); yellow, STAT6 $^{-/-}$ given FPV-HIV (which represents permanent STAT6 signaling inhibition condition); green, WT BALB/c given FPV-HIV-IL-4R antagonist vaccine (which represents transient IL-4/IL-13/STAT6 signaling inhibition condition); grey, IL-13 $^{-/-}$ given FPV-HIV (which represents permanent IL-13 inhibition condition); and purple, WT BALB/c given FPV-HIV-IL-13R α 2 adjuvanted vaccine (which represents transient IL-13 sequestration/inhibition condition). Lung NKp46 $^{+}$ ILC1/ILC3 were gated as CD45 $^{+}$ FSC low SSC low lineage $^{-}$ IL-33R/ST2 $^{-}$ NKp46 $^{+}$ cells. The FACS plots in each panel indicate the percentage of NKp46 $^{+}$ ILC1/ILC3 expressing IL-13R α 2 (a), IL-13R α 1 (b), IL-4R α (c), and γ C chain (d). The brackets below the cell percentage indicate the number of cells in each gate. The graph in each panel represents the number of NKp46 $^{+}$ ILC1/ILC3 expressing the different receptors 24 h post vaccination back calculated to CD45 $^{+}$ population, as described in the materials and methods. The error bars represent the mean and standard deviation (s.d.). The p values were calculated using one-way ANOVA using Tukey's multiple comparisons test and unpaired t -test. * $p < 0.05$, ** $p < 0.01$, **** $p < 0.0001$. Experiments were repeated a minimum of 3 times.

3.5. rFPV and rVV Vaccinated Lung cDCs and pDC Exhibited Uniquely Differential IL-4/IL-13 Receptor Expression Profiles 24–72 h Post-Delivery

We have previously shown that the nature and replication status of a viral vector can significantly alter the ILC2-derived IL-13 level at the vaccination and can modulate lung DC recruitment [30]. Moreover, a low IL-13 environment at the vaccination site can recruit enhanced cDC leading to CD8⁺ T cells of higher avidity [31,32], whilst IL-13 was necessary for effective antibody differentiation [33,51]. Knowing that pDCs play a role in effective antibody differentiation [52,53], in this study IL-4/IL-13 receptor regulation on cDCs and pDCs were also assessed 24–72 h post rFPV and rVV vaccination (high and low IL-13 conditions), as described in Figure S8. The results indicated that compared to rFPV, known to induce low ILC2-derived IL-13 [24,30], rVV induced considerably elevated ILC2-derived IL-13 at the lung mucosae by an ST2/IL-33R⁻ ILC subset, 24 h post vaccination ($p < 0.0001$) (Figure 7a). There was significant regulation of the different IL-4/IL-13 receptors on both cDC and pDC at early stages of vaccination. Interestingly, although the percentage of cDCs expressing IL-13R α 2 was much greater 24–48 h (90%) compared to 72 h post rFPV delivery (~80%) ($p < 0.0001$) (Figure 7b), the IL-4R α and IL-13R α 1 on cDC were significantly up-regulated only after 48 h (24 vs. 48 h and 24 vs. 72 h $p < 0.0001$) (Figure 7b). In contrast, post rVV vaccination, significantly elevated and sustained IL-13R α 2 expression (99%) was detected throughout the time course (Figure 7c), whilst the IL-13R α 1/IL-4R α expression trends were very similar to rFPV vaccination (Figure 7c). Notably, at these time points γ C receptor, which forms the IL-4 type I receptor complex (IL-4R α and γ C), was not expressed or regulated at 72 h post vaccination (Figure S9).

IL-13R α 2 densities, 24 to 72 h post rFPV vaccination, were down regulated (Figure S10a), whilst the opposite was observed with IL-13R α 1 and IL-4R α (Figure S10b,c). In contrast, post rVV vaccination down-regulation of both IL-13R α 2 and IL-13R α 1 densities at 48 h (24 vs. 48 h $p < 0.0001$), followed by an up-regulation at 72 h, comparable to 24 h (Figure S10d,e) and a gradual but significant increase in the IL-4R α densities, were detected over time (24 vs. 48 h $p = 0.0127$, 48 vs. 72 h and 24 vs. 72 h $p < 0.0001$) (Figure S10f). Interestingly, on cDC the IL-13R α 2 densities were approximately ten times greater than IL-13R α 1 and IL-4R α .

The IL-13R α 2 expression on pDCs post rFPV vaccination was found to be in the order of (24 > 48 < 72 h) (24 vs. 48 h and 48 vs. 72 h $p < 0.0001$) (Figure 7d), whereas rVV showed a significant up-regulation of IL-13R α 2, both at 48 and 72 h, compared to 24 h post-delivery (24 < 48 \leq 72 h) (24 vs. 48 h and 24 vs. 72 h $p < 0.0001$) (Figure 7e). Interestingly, very a low number of rFPV vaccinated pDCs expressed IL-4R α , IL-13R α 1, and γ C at 24 h and 48 h ($\geq 3\%$), and no detectable expression was observed at 72 h post-delivery (Figure 7d and Figure S11a). In contrast, significant up regulations of IL-4R α and IL-13R α 1 were detected on rVV vaccinated lung pDCs 48 to 72 h post-delivery (20–80%), where a very high proportion of pDCs expressed IL-13R α 1 (24 vs. 48 and 24 vs. 72 h $p < 0.0001$) and IL-4R α (24 vs. 48 $p < 0.0001$ and 24 vs. 72 h $p = 0.0003$) compared to at 24 h ($\geq 2\%$) (Figure 7e). However, less than 2% of rVV vaccinated pDCs expressed γ C at 24 h, and no detectable expression was found at other time points (Figure 7e and Figure S11b).

Post rFPV vaccination, a significant decrease in IL-13R α 2 (24 vs. 48 h $p = 0.0002$; 24 vs. 72 h $p = 0.0003$), IL-13R α 1 (24 vs. 48 h and 24 vs. 72 h $p = 0.0284$), and IL-4R α densities (24 vs. 48 h and 24 vs. 72 h $p = 0.0277$) was observed over time (Figure S12a). In contrast, rVV vaccinated pDCs showed a significantly elevated IL-13R α 2 density at 72 h (24 vs. 72 h $p < 0.0001$), including the IL-13R α 1 (24 vs. 48 h $p = 0.0002$; 24 vs. 72 h $p < 0.0001$) and IL-4R α densities (24 vs. 48 h and 24 vs. 72 h $p < 0.0001$) (Figure S12b). Interestingly, the density of IL-13R α 2 on rVV vaccinated pDC was approximately 10 times greater than that of IL-13R α 1 and IL-4R α .

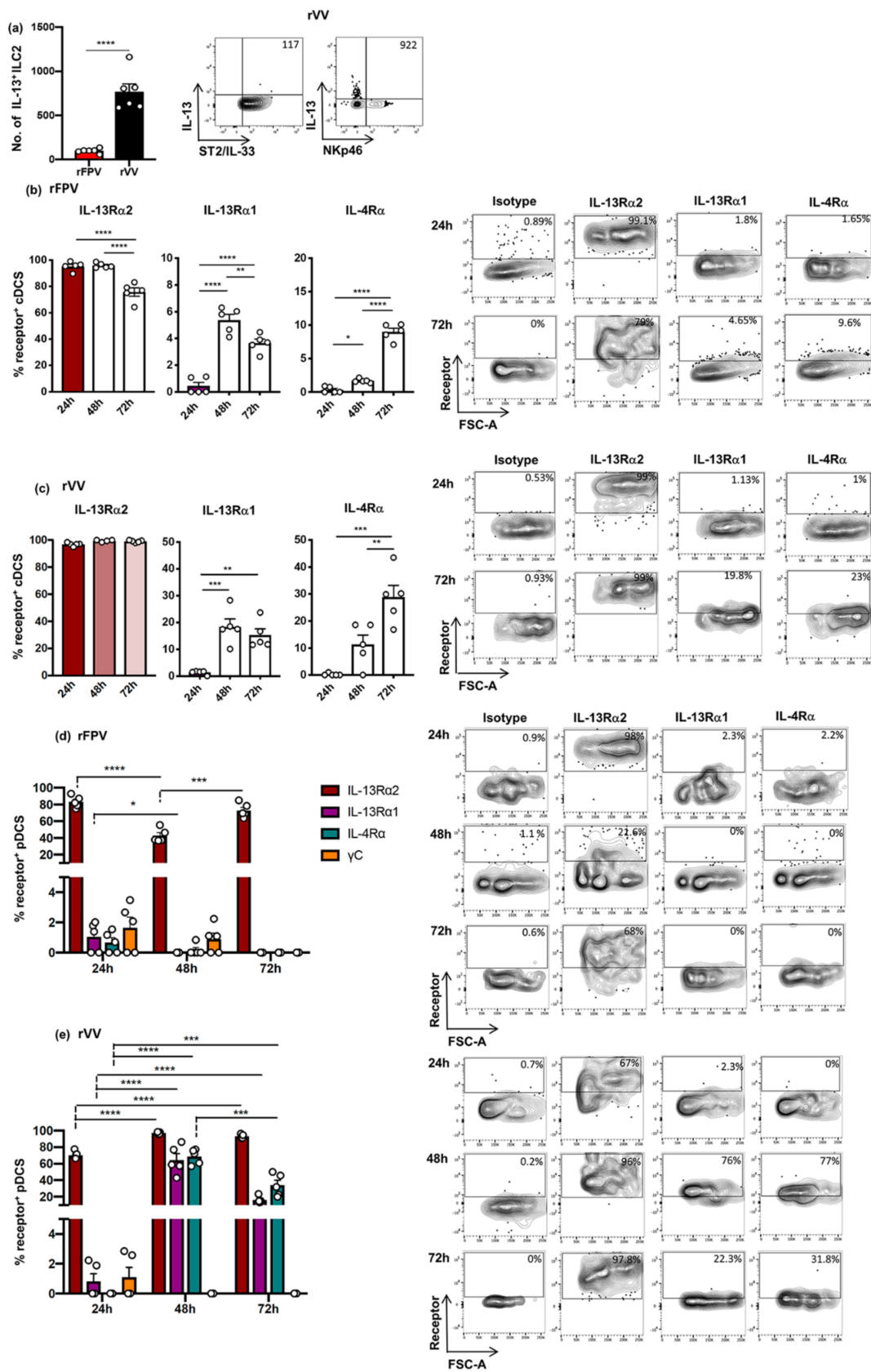


Figure 7. Evaluation of lung ILC2-derived IL-13 expression and lung cDCs and pDCs expressing IL-4/IL-13 receptors, following intranasal rFPV and rVV vaccination. BALB/c mice (n = 6 per group) were immunized i.n. with FPV-HIV or VV-HIV, 24 h post vaccination single cell suspensions from lungs were prepared and stained for lineage⁻ ST2/IL-33⁺ and

lineage⁻ ST2/IL-33⁻ NKp46⁻ ILC2s, and their IL-13 expression was assessed using flow cytometry, as described in the materials and methods. Graphs show (a) the number of lineage⁻ ST2/IL-33R⁺ and lineage⁻ ST2/IL-33⁻ NKp46⁻ ILC2s expressing IL-13, 24 h post rFPV and rVV vaccination (left panel). (a) Representative FACS plots show the average number of lineage⁻ ST2/IL-33R⁺ and lineage⁻ ST2/IL-33⁻ NKp46⁻ ILC2s expressing IL-13 following rVV vaccination (right panel). BALB/c lungs (n = 5 per vaccine group) were harvested at 24 h, 48 h, or 72 h post rFPV or rVV delivery. Single cell suspensions were prepared and stained for MHC-II⁺ CD11c⁺ CD11b⁺ CD103⁻ cDCs and IL-4/IL-13 receptors and the expression on lung cDCs was assessed using flow cytometry, as described in the materials and methods. Bar graphs (left panel) and representative flow cytometry plots (right panel) show IL-13Rα2, IL-13Rα1, and IL-4Rα expression following vaccination with (b) rFPV and (c) rVV vaccination. Another set of single cell suspensions from the same vaccinated animals were prepared and stained for IL-4/IL-13 receptors on lung MHC-II⁺ CD11c⁺ CD11b⁻ B220⁺ pDCs. Bar graphs (left panel) and representative flow cytometry plots (right panel) show IL-13Rα2, IL-13Rα1, IL-4Rα, and γC expression at 24 h, 48 h, and 72 h post (d) rFPV and (e) rVV vaccination. Error bars represent standard error of mean (SEM), and *p* values were calculated using one-way ANOVA followed by Tukey's multiple comparison test (black lines) and unpaired non-parametric student's *t* test (grey lines). * *p* < 0.05, ** *p* < 0.01, *** *p* < 0.001, **** *p* < 0.0001. Experiments with each vector were repeated minimum a 2–3 times.

4. Discussion

The current findings revealed that, 24 h post intranasal viral vector vaccination, the expression of IL-13 and IFN-γ in lung ILC2 and ILC1/ILC3 subsets were differentially regulated under transient versus permanent blockage of IL-13 and STAT6. This was governed by the regulation of IL-4/IL-13 receptors (type I γC/IL-4Rα, type II IL-4Rα/IL-13Rα1 IL-4 receptor complexes, and IL-13Rα2) on ST2/IL-33R⁺ ILC2 and NKp46⁻ ILC1/ILC3. Specifically, unlike the IL-13 inhibitory conditions, the disruption of STAT6 signaling induced differential IL-13Rα2 expression on ST2/IL-33R⁺ ILC2 and NKp46⁻ ILC1/ILC3, alluding to regulation of IL-13 by IL-13Rα2, under certain conditions (Table 1). Animals given the FPV-HIV-IL-4R antagonist vaccination (which has shown low or no ILC2-derived IL-13 expression [24]), induced an elevated number of ST2/IL-33R⁺ ILC2 expressing IL-13Rα2, whilst, STAT6^{-/-} mice given the unadjuvanted vaccine showed elevated ST2/IL-33R⁺ ILC2-derived IL-13 and very low IL-13Rα2 expression (Table 1). Knowing that IL-13Rα2 is the high affinity receptor for IL-13 (works/signals under low IL-13 on lung DCs) [14], these observations jointly implied the possible co-regulation of ILC2-derived IL-13 and IL-13Rα2 at the vaccination site (Figure 8 and Figure S14), unlike IL-13Rα1 (as expression of the latter was similar between the three groups tested (Figure 2)). Moreover, the down-regulation of both IFN-γ and IL-13Rα2 in STAT6^{-/-} NKp46⁻ ILC1/ILC3 given the unadjuvanted vaccine, and the opposing effect (up-regulation of IFN-γ and IL-13Rα2) observed in NKp46⁻ ILC1/ILC3s, when WT BALB/c mice were given the FPV-HIV-IL-4R antagonist adjuvanted vaccine (transient inhibition of STAT6), indicated that at the lung mucosae the IL-13 and IFN-γ balance was likely inter-regulated by different ILCs (Figure 8 and Figure S14). Interestingly, IL-13^{-/-} mice given the FPV-HIV (which has shown low or no ILC2-derived IL-13 expression [24]), showed elevated expression of IFN-γ by NKp46⁻ ILC1/ILC3, whereas BALB/c mice given the FPV-HIV-IL-13Rα2 adjuvanted vaccine showed reduced ST2/IL-33R⁺ ILC2-driven IL-13, as well as NKp46⁻ ILC1/ILC3-driven IFN-γ expression (Table 1). It is now well recognized that IL-13 can modulate IFN-γ expression [54,55], and our recent findings also showed that ST2/IL-33R⁺ ILC2 can express elevated IFN-γR (Figure S13) (Jeason et al. in preparation). Moreover, an inverse relationship between IL-13Rα2 and IFN-γR expression on lung DCs was recently established following FPV-HIV vaccination [14], associated with low ILC2-derived IL-13 [24,30]. Thus, taken together our findings indicated that redundancies built into the immune system employ a range of regulatory mechanisms to control the balance of ST2/IL-33R⁺ ILC2-driven IL-13 and NKp46⁻ ILC1/ILC3-driven IFN-γ at the vaccination site. Specifically, this balance was likely inter-regulated by IL-13Rα2/IFN-γR on ST2/IL-33R⁺ ILC2 and NKp46⁻ ILC1/ILC3 (Figure 8 and Figure S14).

Table 1. Summary of ILC-derived cytokine and IL-13R α 2 expression on ILC 24 h post intranasal rFPV vaccination under different IL-4/IL-13 signaling conditions and resulting adaptive immune outcomes *.

Condition	IL-13 (by ILC2)	IL-13R α 2 (ILC2)	IL-13R α 2 (NKp46 ⁻ ILC)	IL-13R α 2 (NKp46 ⁺ ILC)	STAT6 Signalling	IFN- γ Level (NKp46 ⁻ ILC)	IFN- γ Level (NKp46 ⁺ ILC)	T Cell Avidity *	Antibody Differentiation *
Control	+++	+++	+++	+++	✓	+++	+++	+++	++++
◇IL-4R antagonist	±	+++++	+++++	+++	⊗	+++++	+++	+++++	++++
◇STAT6 ^{-/-}	+++++	+	+++	++	⊗	+	+	++	+++++
IL-13R α 2 vaccine	±	+++	+++	+++	✓	+	+	+++++	±
IL-13 ^{-/-}	-	-	+++++	++	✓	++	+++	+++++	+

Symbols represent: - absent or below detection, ± week or very low, + low, ++ medium, +++ moderate, ++++ high, +++++ very high, ✓ signaling present, ⊗ signaling absent (permanently or transiently). * Note that the adaptive immune outcomes were published in the following articles [32–37]. ◇IL-4R antagonist prime-boost vaccination induced high avidity in both effector and memory T cells (outcomes were confirmed both in mice and macaques [33–35]) together with elevated IgG1/IgG2a antibodies, whereas STAT6^{-/-} mice given unadjuvanted strategy generated high avidity memory T cells (not effector) and elevated IgG2a (very low IgG), compared to the WT BALB/c given the unadjuvanted strategy [33,36,37].

Our HIV prime-boost vaccine studies have demonstrated that IL-13 signaling via an STAT6 independent pathway, most likely IL-13R α 2, was detrimental for effective IgG1 to IgG2a antibody differentiation following viral vector-based vaccination [33,37] (Table 1). Specifically, IL-4R antagonist vaccination (which interrupted the STAT6 signaling) induced low ILC2-derived IL-13 and elevated NKp46^{+/-} ILC1/ILC3-derived IFN- γ expression at the vaccination site 24 h post-delivery [24]. Interestingly, the role of IFN- γ in effective antibody maturation/development has been well-documented [38–42]. Remarkably, studies have also shown that the IL-13R α 2 cytoplasmic domain can bind to IL-4R α to prevent STAT6 signaling [17], and IL-4R α /STAT6 signaling can inhibit IFN- γ expression in CD4⁺ T cells [56]. Recently, IL-13 signaling via IL-13R α 2, leading to expression of TGF- β 1 in DCs [14], and association of TGF- β as a key regulator of IgG2a antibody induction, have also been reported [57–59]. Therefore, in the context of IL-4R antagonist adjuvanted vaccination (transient blockage of IL-13, and STAT6 signaling) the observed IL-4/IL-13 receptor regulation patterns on ILC also suggested a possible autocrine regulation of ILC2-derived IL-13 in the milieu via IL-13R α 2, as well as the activation of IL-13R α 2 on ILC1/ILC3 to regulate the elevated NKp46⁻ ILC1/ILC3-derived IFN- γ expression (Figure S14). In contrast, in STAT6^{-/-} mice given the unadjuvanted vaccine, receptor regulation patterns indicated sequestration of elevated ST2/IL-33R⁺ ILC2-driven IL-13 by NKp46⁻ ILC1/ILC3 IL-13R α 2, preventing IL-13R α 2 signaling and NKp46⁻ ILC1/ILC3-derived IFN- γ expression (Figure S14). This was similar to what was recently reported in DC under different IL-13 conditions [14]. Interestingly, in this study, following rFPV vaccination, enhanced IL-13R α 2 expression on pDC with no significant IL-13R α 1/IL-4R α regulation 24–72 h post-delivery was also observed, unlike rVV vaccination (high IL-13 conditions) [14]. Knowing the association of pDCs [52,53] in effective antibody maturation/development, collectively, the current findings once again indicated that IL-13R α 2 plays an important role at the first line of defense, not only at the DC [14] but also ILC level to regulate/maintain the IL-13 and IFN- γ balance at the vaccination site (Figure 8), responsible for diverse adaptive immune outcomes (Table 1).

Intriguingly, the regulation of IL-4/IL-13 receptors on lung ILCs was significantly different under STAT6 compared to IL-13 inhibitory conditions. Although 24 h post FPV-HIV-IL-13R α 2 adjuvanted or unadjuvanted vaccination type I (γ C/IL-4R α) IL-4 receptor complex was regulated on WT BALB/c ST2/IL-33R⁺ ILC2, interestingly, IL-13 receptors (IL-13R α 1 or IL-13R α 2) were not regulated. However, ST2/IL-33R⁺ ILC2 obtained from IL-13^{-/-} mice given the unadjuvanted vaccination showed regulation of type I (γ C/IL-4R α) and type II (IL-4R α /IL-13R α 1) IL-4 receptor complexes, but showed no detectable expression of IL-13R α 2 or IL-4. Moreover, the expression hierarchy of NKp46⁻ ILC1/ILC3-driven IFN- γ in these mice was in the order: BALB/c unadjuvanted > IL-13^{-/-} unadjuvanted > BALB/c IL-13R α 2 adjuvanted vaccinated (Table 1). Therefore, the observed cytokine and receptor expression profiles suggest that, as IL-4/IL-13 have overlapping specific-

ties, under IL-13^{-/-} conditions, IL-4 expressed by other cells at the lung mucosae may interact with type I and/or II IL-4 receptor complexes on ILC2 to compensate for the loss of IL-13 in the milieu to regulate the ILC/cytokine balance at the vaccination site (e.g., IL-13/IFN- γ). The above findings further corroborated our notion that at the early stages of vaccination, IL-13 is likely the master sensor/regulator of lung ST2/IL-33R⁺ ILC2 and NKp46⁻ ILC1/ILC3 activity/function.

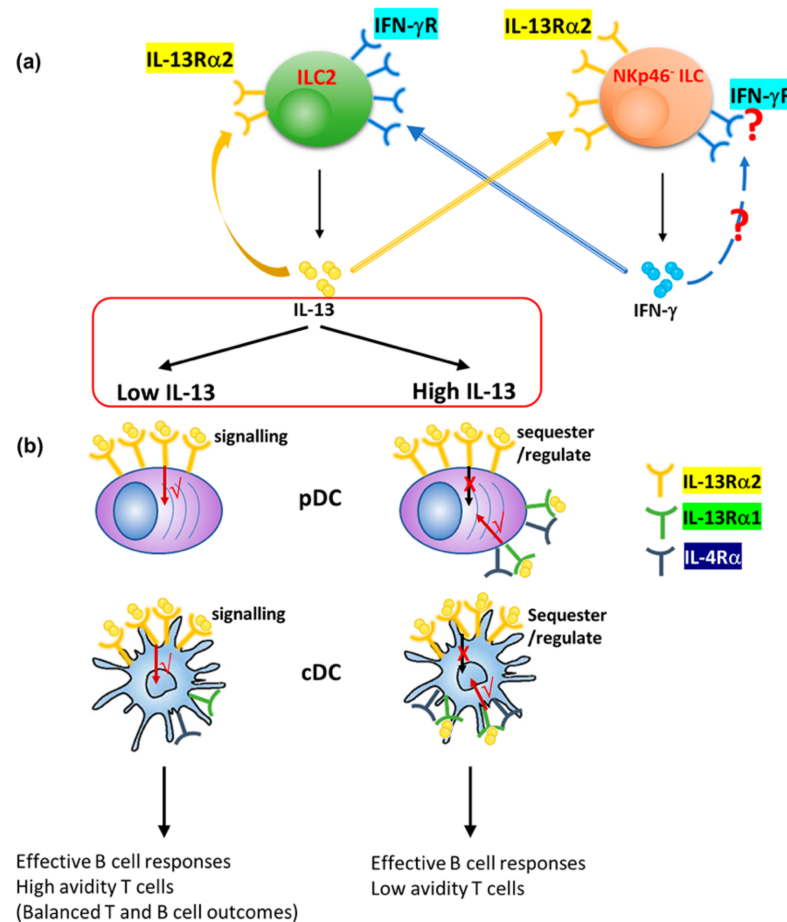


Figure 8. Schematic diagram showing the proposed co-regulation of ILC2-derived IL-13, inter-regulation of ILC2 and ILC1/ILC3 and DC under high and low IL-13. (a) At 24 h post viral FPV-HIV vaccination, lung IL-33R/ST2⁻ ILC2-derived IL-13 and IL-13R α 2 were co-regulated. Moreover, the ILC2-derived IL-13 and NKp46⁻ ILC1/ILC3-derived IFN- γ were also inter-regulated by their respective receptors (IFN- γ R and IL-13R α 2) present on these ILCs. Taken together our findings indicate that at the early stages of vaccination, IL-13 is the master regulator of different ILC subsets. However, whether there is regulation of IFN- γ via IFN- γ R on ILC1/ILC3 warrants further investigation. Moreover, see Figure S8 for STAT6 and IL-13 transient versus permanent inhibition scenarios. (b) Under low (rFPV) and high (rVV) IL-13 conditions DCs are differentially regulated. Under low IL-13 conditions, IL-13 signals via the high affinity receptor IL-13R α 2 on pDCs and cDCs, inducing effective B cell (e.g., differentiated antibody responses) as well as high avidity/polyfunctional T cells responses [32,33,36,37]. Under high IL-13 conditions, IL-13 signals via the low affinity Type II IL-4 receptor IL-13R α 1/IL-4R α complex, on pDCs and cDCs, while IL-13R α 2 sequesters/regulates excess IL-13 at the vaccination site maintaining homeostasis, resulting in effective B cell but not T cell outcomes.

On NKp46⁺ ILC1/ILC3s the expression patterns of IL-4/IL-13 receptors were vastly different compared to the other two ILC subsets. The stable IL-13R α 2 expression on NKp46⁺ ILC1/ILC3 under the transient and control vaccination conditions indicated that these cells were not involved in regulation of ILC2 and NKp46⁻ ILCs, but were likely

associated with maintenance of IL-13 homeostasis at the lung mucosae, similar to what has been observed in lung DC under high IL-13 conditions [14], and under IL-13 mediated chronic inflammatory conditions [60,61]. Furthermore, the low IFN- γ expression and minimal regulation of IL-13R α 2 at the early stages of intranasal viral vector vaccination was suggestive of the noninvolvement NKp46⁺ ILC1/ILC3s in the regulation of lung ST2/IL-33R⁺ ILC2.

Unlike rFPV associated with low ILC2-derived, rVV vaccination, which induced significantly elevated ILC2-derived IL-13 (the highest compared to all previously tested viral vectors) [30], showed elevated expression of the high affinity IL-13 receptor IL-13R α 2 on lung DCs 24–72 h post-delivery, including significant up-regulation of the low affinity Type II IL-4R α /IL-13R α 1 complex at 48–72 h. These receptor regulation patterns once again provoked the notion that under high IL-13, IL-13R α 2 likely sequestered excess IL-13 (noting that rVV is a replicating vector), whilst signaling took place via the low affinity IL-4R α /IL-13R α 1 complex (which works under high IL-13 conditions) (Figure 8). These findings are highly consistent with our recent observations, where low and high IL-13 conditions showed differential regulation of IL-13R α 2 on DC [14]. These uniquely different early events in the innate immune compartment may explain “how and why” (i) in a prime-boost vaccination modality, rFPV prime can generate high avidity T cells, unlike rVV [62]; and (ii) the order of vector delivery significantly impacts vaccine-specific adaptive immune outcomes [63,64]. Moreover, the observed IL-13/IL-13R α 2 regulation patterns on ILC and DC at the vaccination site may explain why a more attenuated and unrelated viral vector to the host may help induce a higher quality vaccine-specific T cell immunity. Specifically, why rFPV and its relative, canarypox virus prime modalities, may have the capacity to induce more effective immune outcomes than other pox viral vectors [34,63–65], given that priming creates the initial antigen-specific T cell population, which gets expanded during the booster vaccination [32,33].

5. Conclusions

Collectively, our findings reveal that 24 h post intranasal viral vector vaccination, lung ILC2-derived IL-13 is regulated in an autocrine fashion via IL-13R α 2, and that most likely there is inter-regulation of ILC2-derived IL-13 and NKp46[−] ILC1/ILC3-derived IFN- γ by their respective receptors (IFN- γ R and IL-13R α 2) present on ILC (Figure 8). Specifically, at the early stages of viral vector vaccination: (i) IL-13 is likely the master regulator of ILC2 and NKp46[−] ILC1/ILC3, as well as DC, and responsible for shaping the downstream adaptive immune outcomes (Table 1); and (ii) IL-13R α 2 is the key IL-13 regulator of both lung ILC and DCs. Thus, taken together with our previous findings, we propose that the IL-13R α 2 and IFN- γ R receptor regulation process at the ILC and DC level may play an important role in shaping not only the T cell but also B cell immune outcomes (Table 1), in a vaccine vector, adjuvant, and a route dependent manner; which warrants further investigation.

Supplementary Materials: The following are available online at <https://www.mdpi.com/article/10.3390/vaccines9050440/s1>, Figure S1: Gating strategy used to assess ILC subsets and their cytokine and IL-13/IL-4 receptor expression; Figure S2: Evaluation of type I (γ C chain and IL-4R α) and type II (IL-4R α and IL-13R α 1) IL-4 receptor complexes and IL-13R α 2 expression on ILC following intranasal rFPV vaccination; Figure S3: IL-13R α 2, IL-13R α 1, IL-4R α , and γ C receptor densities on ILC2 following rFPV vaccination—(permanent vs transient inhibition of STAT6 signaling); Figure S4: IL-13R α 2, IL-13R α 1, IL-4R α , and γ C receptor densities on lineage[−] IL-33R/ST2[−] NKp46[−] ILC1/ILC3 following rFPV vaccination—(permanent vs transient inhibition of STAT6 signaling); Figure S5: IL-13R α 2, IL-13R α 1, IL-4R α , and γ C receptor densities on ILC2 following unadjuvanted and IL-13R α 2 adjuvanted vaccination—(permanent vs transient inhibition of IL-13 signaling); Figure S6: IL-13R α 2, IL-13R α 1, IL-4R α , and γ C receptor densities on lineage[−] IL-33R/ST2[−] NKp46[−] ILC1/ILC3 following unadjuvanted and IL-13R α 2 adjuvanted vaccination—(permanent vs transient inhibition of IL-13 signaling); Figure S7: Results from Figures 1–6 presented in the form of percentage out of CD45⁺ cells; Figure S8: Flow cytometry gating for evaluation of IL-4/IL-13 receptors on lung cDCs and

pDCs following i.n. viral vector-based vaccination; Figure S9: Evaluation of γ c expression on lung cDCs at 24, 48 and 72 h following viral vector-based vaccination; Figure S10: Evaluation of IL-13R α 2, IL-13R α 1, and IL-4R α receptor densities on lung cDCs at 24, 48 and 72 h following viral vector-based vaccination; Figure S11: Evaluation of γ c expression on lung pDCs at 24, 48 and 72 h following viral vector-based vaccination; Figure S12: Evaluation of IL-13R α 2, IL-13R α 1, and IL-4R γ receptor densities on lung pDCs at 24, 48 and 72 h following viral vector-based vaccination; Figure S13: Evaluation of IFN- γ R on lung ST2/IL-33R⁺ ILC2, 24 h post FPV-HIV vector vaccination; Figure S14: Schematic diagram showing the proposed co-regulation of ILC2-derived IL-13 and inter-regulation of ILC2 and ILC1/ILC3 under permanent vs transient STAT6 and IL-13 inhibition conditions.

Author Contributions: Z.L. conducted ILC experiments, data analysis, figures, and the preparation of the manuscript. S.R. conducted the DC experiments, related data analysis, and figures. C.R. conceived the idea, helped design the experiments and with critical evaluation and preparation of the manuscript. All authors have read and agreed to the published version of the manuscript.

Funding: This work was supported by the Australian Centre for HIV and Hepatitis Virology Research (ACH2), ANU Connect Ventures grant award DTF 230, and Australian National Health and Medical Research Council (NHMRC) development grant APP1136351 awarded to C.R. Z.L. currently supported by The Coalition for Epidemic Preparedness Innovations grant awarded to C.R.

Institutional Review Board Statement: All animals were maintained, and experiments were performed in accordance with the Australian National Health and Medical Research Council (NHMRC) guidelines within the Australian Code of Practice for the Care and Use of Animals for Scientific Purposes. The animal ethics were approved by The Australian National University's, Animal Experimentation and Ethics Committee (AEEC). Protocol numbers A2014/14, and A2017/15.

Informed Consent Statement: Not applicable.

Data Availability Statement: The authors declare that all data supporting the findings of this study are available within the paper and supplementary files.

Acknowledgments: The authors would like to thank Ronald J. Jackson for constructing the IL-4R antagonist and IL-13R α 2 adjuvanted vaccines. Michael Devoy and Harpreet Vohra at the MCRF/JCSMR ANU for their technical assistance with flow cytometry.

Conflicts of Interest: The authors declare no commercial or financial conflict of interests.

References

1. Hurdalay, R.; Brombacher, F. The role of IL-4 and IL-13 in cutaneous Leishmaniasis. *Immunol. Lett.* **2014**, *161*, 179–183. [[CrossRef](#)] [[PubMed](#)]
2. Maizels, R.M.; Hewitson, J.P.; Smith, K.A. Susceptibility and immunity to helminth parasites. *Curr. Opin. Immunol.* **2012**, *24*, 459–466. [[CrossRef](#)] [[PubMed](#)]
3. Paul, W.E.; Zhu, J. How are T(H)2-type immune responses initiated and amplified? *Nat. Rev. Immunol.* **2010**, *10*, 225–235. [[CrossRef](#)] [[PubMed](#)]
4. Bao, K.; Reinhardt, R.L. The differential expression of IL-4 and IL-13 and its impact on type-2 immunity. *Cytokine* **2015**, *75*, 25–37. [[CrossRef](#)]
5. Catley, M.C.; Coote, J.; Bari, M.; Tomlinson, K.L. Monoclonal antibodies for the treatment of asthma. *Pharmacol. Ther.* **2011**, *132*, 333–351. [[CrossRef](#)]
6. Jiang, S.; Dong, C. A complex issue on CD4(+) T-cell subsets. *Immunol. Rev.* **2013**, *252*, 5–11. [[CrossRef](#)]
7. Tabata, Y.; Khurana Hershey, G.K. IL-13 receptor isoforms: Breaking through the complexity. *Curr. Allergy Asthma Rep.* **2007**, *7*, 338–345. [[CrossRef](#)]
8. McCormick, S.M.; Heller, N.M. Commentary: IL-4 and IL-13 receptors and signaling. *Cytokine* **2015**, *75*, 38–50. [[CrossRef](#)]
9. Junttila, I.S.; Creusot, R.J.; Moraga, I.; Bates, D.L.; Wong, M.T.; Alonso, M.N.; Suhoski, M.M.; Lupardus, P.; Meier-Schellersheim, M.; Engleman, E.G.; et al. Redirecting cell-type specific cytokine responses with engineered interleukin-4 superkines. *Nat. Chem. Biol.* **2012**, *8*, 990–998. [[CrossRef](#)]
10. Munitz, A.; Brandt, E.B.; Mingler, M.; Finkelman, F.D.; Rothenberg, M.E. Distinct roles for IL-13 and IL-4 via IL-13 receptor alpha1 and the type II IL-4 receptor in asthma pathogenesis. *Proc. Natl. Acad. Sci. USA* **2008**, *105*, 7240–7245. [[CrossRef](#)]
11. Murata, T.; Husain, S.R.; Mohri, H.; Puri, R.K. Two different IL-13 receptor chains are expressed in normal human skin fibroblasts, and IL-4 and IL-13 mediate signal transduction through a common pathway. *Int. Immunol.* **1998**, *10*, 1103–1110. [[CrossRef](#)]
12. Murata, T.; Noguchi, P.D.; Puri, R.K. IL-13 induces phosphorylation and activation of JAK2 Janus kinase in human colon carcinoma cell lines: Similarities between IL-4 and IL-13 signaling. *J. Immunol. Baltim. Md. 1950* **1996**, *156*, 2972–2978.

13. Lupardus, P.J.; Birnbaum, M.E.; Garcia, K.C. Molecular basis for shared cytokine recognition revealed in the structure of an unusually high affinity complex between IL-13 and IL-13Ralpha2. *Struct. Lond. Engl.* **1993**, *18*, 332–342. [[CrossRef](#)]
14. Roy, S.; Liu, H.-Y.; Jaeson, M.I.; Deimel, L.P.; Ranasinghe, C. Unique IL-13R α 2/STAT3 mediated IL-13 regulation detected in lung conventional dendritic cells, 24 h post viral vector vaccination. *Sci. Rep.* **2020**, *10*, 1017. [[CrossRef](#)]
15. Murata, T.; Obiri, N.I.; Puri, R.K. Human ovarian-carcinoma cell lines express IL-4 and IL-13 receptors: Comparison between IL-4 and IL-13-induced signal transduction. *Int. J. Cancer* **1997**, *70*, 230–240. [[CrossRef](#)]
16. Wood, N.; Whitters, M.J.; Jacobson, B.A.; Witek, J.; Sypek, J.P.; Kasaian, M.; Eppihimer, M.J.; Unger, M.; Tanaka, T.; Goldman, S.J.; et al. Enhanced interleukin (IL)-13 responses in mice lacking IL-13 receptor alpha 2. *J. Exp. Med.* **2003**, *197*, 703–709. [[CrossRef](#)]
17. Rahaman, S.O.; Sharma, P.; Harbor, P.C.; Aman, M.J.; Vogelbaum, M.A.; Haque, S.J. IL-13R(alpha)2, a decoy receptor for IL-13 acts as an inhibitor of IL-4-dependent signal transduction in glioblastoma cells. *Cancer Res.* **2002**, *62*, 1103–1109.
18. Rahaman, S.O.; Vogelbaum, M.A.; Haque, S.J. Aberrant Stat3 signaling by interleukin-4 in malignant glioma cells: Involvement of IL-13Ralpha2. *Cancer Res.* **2005**, *65*, 2956–2963. [[CrossRef](#)]
19. Ko, C.W.; Cuthbert, R.J.; Orsi, N.M.; Brooke, D.A.; Perry, S.L.; Markham, A.F.; Coletta, P.L.; Hull, M.A. Lack of interleukin-4 receptor alpha chain-dependent signalling promotes azoxymethane-induced colorectal aberrant crypt focus formation in Balb/c mice. *J. Pathol.* **2008**, *214*, 603–609. [[CrossRef](#)]
20. Nakashima, H.; Terabe, M.; Berzofsky, J.A.; Husain, S.R.; Puri, R.K. A Novel Combination Immunotherapy for Cancer by IL-13R α 2-Targeted DNA Vaccine and Immunotoxin in Murine Tumor Models. *J. Immunol. Baltim. Md. 1950* **2011**, *187*, 4935–4946. [[CrossRef](#)]
21. Fujisawa, T.; Joshi, B.H.; Puri, R.K. IL-13 regulates cancer invasion and metastasis through IL-13Ralpha2 via ERK/AP-1 pathway in mouse model of human ovarian cancer. *Int. J. Cancer* **2012**, *131*, 344–356. [[CrossRef](#)] [[PubMed](#)]
22. Papageorgis, P.; Ozturk, S.; Lambert, A.W.; Neophytou, C.M.; Tzatsos, A.; Wong, C.K.; Thiagalingam, S.; Constantinou, A.I. Targeting IL13Ralpha2 activates STAT6-TP63 pathway to suppress breast cancer lung metastasis. *Breast Cancer Res. BCR* **2015**, *17*, 98. [[CrossRef](#)] [[PubMed](#)]
23. Bartolome, R.A.; Garcia-Palmero, I.; Torres, S.; Lopez-Lucendo, M.; Balyasnikova, I.V.; Casal, J.I. IL13 Receptor alpha2 Signaling Requires a Scaffold Protein, FAM120A, to Activate the FAK and PI3K Pathways in Colon Cancer Metastasis. *Cancer Res.* **2015**, *75*, 2434–2444. [[CrossRef](#)] [[PubMed](#)]
24. Li, Z.; Jackson, R.J.; Ranasinghe, C. Vaccination route can significantly alter the innate lymphoid cell subsets: A feedback between IL-13 and IFN- γ . *Jpn. Vaccines* **2018**, *3*, 10. [[CrossRef](#)]
25. Li, Z.; Jackson, R.J.; Ranasinghe, C. A hierarchical role of IL-25 in ILC development and function at the lung mucosae following viral-vector vaccination. *Vaccine X* **2019**, *2*, 100035. [[CrossRef](#)]
26. Kim, B.S.; Artis, D. Group 2 innate lymphoid cells in health and disease. *Cold Spring Harb. Perspect. Biol.* **2015**, *7*, a016337. [[CrossRef](#)]
27. Klose, C.S.N.; Artis, D. Innate lymphoid cells control signaling circuits to regulate tissue-specific immunity. *Cell Res.* **2020**, *30*, 475–491. [[CrossRef](#)]
28. Colonna, M. Innate Lymphoid Cells: Diversity, Plasticity, and Unique Functions in Immunity. *Immunity* **2018**, *48*, 1104–1117. [[CrossRef](#)]
29. Bal, S.M.; Golebski, K.; Spits, H. Plasticity of innate lymphoid cell subsets. *Nat. Rev. Immunol.* **2020**, *20*, 552–565. [[CrossRef](#)]
30. Roy, S.; Jaeson, M.I.; Li, Z.; Mahboob, S.; Jackson, R.J.; Grubor-Bauk, B.; Wijesundara, D.K.; Gowans, E.J.; Ranasinghe, C. Viral vector and route of administration determine the ILC and DC profiles responsible for downstream vaccine-specific immune outcomes. *Vaccine* **2019**, *37*, 1266–1276. [[CrossRef](#)]
31. Trivedi, S.; Jackson, R.J.; Ranasinghe, C. Different HIV pox viral vector-based vaccines and adjuvants can induce unique antigen presenting cells that modulate CD8 T cell avidity. *Virology* **2014**, *468–470*, 479–489. [[CrossRef](#)]
32. Ranasinghe, C.; Trivedi, S.; Stambas, J.; Jackson, R.J. Unique IL-13Ralpha2-based HIV-1 vaccine strategy to enhance mucosal immunity, CD8(+) T-cell avidity and protective immunity. *Mucosal Immunol.* **2013**, *6*, 1068–1080. [[CrossRef](#)]
33. Jackson, R.J.; Worley, M.; Trivedi, S.; Ranasinghe, C. Novel HIV IL-4R antagonist vaccine strategy can induce both high avidity CD8 T and B cell immunity with greater protective efficacy. *Vaccine* **2014**, *32*, 5703–5714. [[CrossRef](#)]
34. Khanna, M.; Jackson, R.J.; Alcantara, S.; Amarasena, T.H.; Li, Z.; Kelleher, A.D.; Kent, S.J.; Ranasinghe, C. Mucosal and systemic SIV-specific cytotoxic CD4(+) T cell hierarchy in protection following intranasal/intramuscular recombinant pox-viral vaccination of pigtail macaques. *Sci. Rep.* **2019**, *9*, 5661. [[CrossRef](#)]
35. Li, Z.; Khanna, M.; Grimley, S.L.; Ellenberg, P.; Gonelli, C.A.; Lee, W.S.; Amarasena, T.H.; Kelleher, A.D.; Purcell, D.F.J.; Kent, S.J.; et al. Mucosal IL-4R antagonist HIV vaccination with SOSIP-gp140 booster can induce high-quality cytotoxic CD4+/CD8+ T cells and humoral responses in macaques. *Sci. Rep.* **2020**, *10*, 22077. [[CrossRef](#)]
36. Ranasinghe, C.; Ramshaw, I.A. Immunisation route-dependent expression of IL-4/IL-13 can modulate HIV-specific CD8(+) CTL avidity. *Eur. J. Immunol.* **2009**, *39*, 1819–1830. [[CrossRef](#)]
37. Hamid, M.A.; Jackson, R.J.; Roy, S.; Khanna, M.; Ranasinghe, C. Unexpected involvement of IL-13 signalling via a STAT6 independent mechanism during murine IgG2a development following viral vaccination. *Eur. J. Immunol.* **2018**, *48*, 1153–1163. [[CrossRef](#)]
38. Finkelman, F.D.; Katona, I.M.; Mosmann, T.R.; Coffman, R.L. IFN-gamma regulates the isotypes of Ig secreted during in vivo humoral immune responses. *J. Immunol. Baltim. Md. 1950* **1988**, *140*, 1022–1027.

39. Coutelier, J.P.; Coulie, P.G.; Wauters, P.; Heremans, H.; van der Logt, J.T. In vivo polyclonal B-lymphocyte activation elicited by murine viruses. *J. Virol.* **1990**, *64*, 5383–5388. [[CrossRef](#)]
40. Graham, M.B.; Dalton, D.K.; Giltinan, D.; Braciale, V.L.; Stewart, T.A.; Braciale, T.J. Response to influenza infection in mice with a targeted disruption in the interferon gamma gene. *J. Exp. Med.* **1993**, *178*, 1725–1732. [[CrossRef](#)]
41. van den Broek, M.F.; Muller, U.; Huang, S.; Aguet, M.; Zinkernagel, R.M. Antiviral defense in mice lacking both alpha/beta and gamma interferon receptors. *J. Virol.* **1995**, *69*, 4792–4796. [[CrossRef](#)]
42. Maloy, K.J.; Odermatt, B.; Hengartner, H.; Zinkernagel, R.M. Interferon gamma-producing gammadelta T cell-dependent antibody isotype switching in the absence of germinal center formation during virus infection. *Proc. Natl. Acad. Sci. USA* **1998**, *95*, 1160–1165. [[CrossRef](#)]
43. Molofsky, A.B.; Van Gool, F.; Liang, H.E.; Van Dyken, S.J.; Nussbaum, J.C.; Lee, J.; Bluestone, J.A.; Locksley, R.M. Interleukin-33 and Interferon-gamma Counter-Regulate Group 2 Innate Lymphoid Cell Activation during Immune Perturbation. *Immunity* **2015**, *43*, 161–174. [[CrossRef](#)]
44. Thio, C.L.; Lai, A.C.; Chi, P.Y.; Webster, G.; Chang, Y.J. Toll-like receptor 9-dependent interferon production prevents group 2 innate lymphoid cell-driven airway hyperreactivity. *J. Allergy Clin. Immunol.* **2019**, *144*, 682–697.e9. [[CrossRef](#)]
45. Han, M.; Hong, J.Y.; Jaipalli, S.; Rajput, C.; Lei, J.; Hinde, J.L.; Chen, Q.; Hershenson, N.M.; Bentley, J.K.; Hershenson, M.B. IFN- γ Blocks Development of an Asthma Phenotype in Rhinovirus-Infected Baby Mice by Inhibiting Type 2 Innate Lymphoid Cells. *Am. J. Respir. Cell Mol. Biol.* **2016**, *56*, 242–251. [[CrossRef](#)]
46. Tomkinson, A.; Duez, C.; Cieslewicz, G.; Pratt, J.C.; Joetham, A.; Shanafelt, M.-C.; Gundel, R.; Gelfand, E.W. A Murine IL-4 Receptor Antagonist That Inhibits IL-4- and IL-13-Induced Responses Prevents Antigen-Induced Airway Eosinophilia and Airway Hyperresponsiveness. *J. Immunol.* **2001**, *166*, 5792–5800. [[CrossRef](#)]
47. Tony, H.P.; Shen, B.J.; Reusch, P.; Sebald, W. Design of human interleukin-4 antagonists inhibiting interleukin-4-dependent and interleukin-13-dependent responses in T-cells and B-cells with high efficiency. *Eur. J. Biochem.* **1994**, *225*, 659–665. [[CrossRef](#)] [[PubMed](#)]
48. Jackson, R.; Boyle, D.; Ranasinghe, C. Heterologous prime-boost regimens in DNA vaccination. In *Methods Molecular Biology*; Springer: Berlin/Heidelberg, Germany, 2014.
49. Townsend, D.G.; Trivedi, S.; Jackson, R.J.; Ranasinghe, C. Recombinant fowlpox virus vector-based vaccines: Expression kinetics, dissemination and safety profile following intranasal delivery. *J. Gen. Virol.* **2017**, *98*, 496–505. [[CrossRef](#)] [[PubMed](#)]
50. Coupar, B.E.H.; Purcell, D.F.J.; Thomson, S.A.; Ramshaw, I.A.; Kent, S.J.; Boyle, D.B. Fowlpox virus vaccines for HIV and SHIV clinical and pre-clinical trials. *Vaccine* **2006**, *24*, 1378–1388. [[CrossRef](#)] [[PubMed](#)]
51. Hamid, Q.; Naseer, T.; Minshall, E.M.; Song, Y.L.; Boguniewicz, M.; Leung, D.Y. In vivo expression of IL-12 and IL-13 in atopic dermatitis. *J. Allergy Clin. Immunol.* **1996**, *98*, 225–231. [[CrossRef](#)]
52. Cerutti, A.; Qiao, X.; He, B. Plasmacytoid dendritic cells and the regulation of immunoglobulin heavy chain class switching. *Immunol. Cell Biol.* **2005**, *83*, 554–562. [[CrossRef](#)]
53. Le Bon, A.; Schiavoni, G.; D'Agostino, G.; Gresser, I.; Belardelli, F.; Tough, D.F. Type I interferons potently enhance humoral immunity and can promote isotype switching by stimulating dendritic cells in vivo. *Immunity* **2001**, *14*, 461–470. [[CrossRef](#)]
54. Albanesi, C.; Fairchild, H.R.; Madonna, S.; Scarponi, C.; De Pita, O.; Leung, D.Y.; Howell, M.D. IL-4 and IL-13 negatively regulate TNF-alpha- and IFN-gamma-induced beta-defensin expression through STAT-6, suppressor of cytokine signaling (SOCS)-1, and SOCS-3. *J. Immunol. Baltim. Md. 1950* **2007**, *179*, 984–992.
55. Xiao, T.; Kagami, S.; Saeki, H.; Sugaya, M.; Kakinuma, T.; Fujita, H.; Yano, S.; Mitsui, H.; Torii, H.; Komine, M.; et al. Both IL-4 and IL-13 inhibit the TNF-alpha and IFN-gamma enhanced MDC production in a human keratinocyte cell line, HaCaT cells. *J. Dermatol. Sci.* **2003**, *31*, 111–117. [[CrossRef](#)]
56. Metwali, A.; Blum, A.; Elliott, D.E.; Weinstock, J.V. Interleukin-4 receptor alpha chain and STAT6 signaling inhibit gamma interferon but not Th2 cytokine expression within schistosome granulomas. *Infect. Immun.* **2002**, *70*, 5651–5658. [[CrossRef](#)]
57. Takeuchi, M.; Alard, P.; Streilein, J.W. TGF-beta promotes immune deviation by altering accessory signals of antigen-presenting cells. *J. Immunol. Baltim. Md. 1950* **1998**, *160*, 1589–1597.
58. Garcia, B.; Rodriguez, R.; Angulo, I.; Heath, A.W.; Howard, M.C.; Subiza, J.L. Differential effects of transforming growth factor-beta 1 on IgA vs. IgG2b production by lipopolysaccharide-stimulated lymph node B cells: A comparative study with spleen B cells. *Eur. J. Immunol.* **1996**, *26*, 2364–2370. [[CrossRef](#)]
59. Arteaga, C.L.; Hurd, S.D.; Winnier, A.R.; Johnson, M.D.; Fendly, B.M.; Forbes, J.T. Anti-transforming growth factor (TGF)-beta antibodies inhibit breast cancer cell tumorigenicity and increase mouse spleen natural killer cell activity. Implications for a possible role of tumor cell/host TGF-beta interactions in human breast cancer progression. *J. Clin. Invest.* **1993**, *92*, 2569–2576.
60. Kawakami, K.; Taguchi, J.; Murata, T.; Puri, R.K. The interleukin-13 receptor alpha2 chain: An essential component for binding and internalization but not for interleukin-13-induced signal transduction through the STAT6 pathway. *Blood* **2001**, *97*, 2673–2679. [[CrossRef](#)]
61. Campbell-Harding, G.; Sawkins, H.; Bedke, N.; Holgate, S.T.; Davies, D.E.; Andrews, A.L. The innate antiviral response upregulates IL-13 receptor alpha2 in bronchial fibroblasts. *J. Allergy Clin. Immunol.* **2013**, *131*, 849–855. [[CrossRef](#)]
62. Wijesundara, D.K.; Ranasinghe, C.; Jackson, R.J.; Lidbury, B.A.; Parish, C.R.; Quah, B.J. Use of an in vivo FTA assay to assess the magnitude, functional avidity and epitope variant cross-reactivity of T cell responses following HIV-1 recombinant poxvirus vaccination. *PLoS ONE* **2014**, *9*, e105366. [[CrossRef](#)]

63. Ranasinghe, C.; Medveczky, J.C.; Woltring, D.; Gao, K.; Thomson, S.; Coupar, B.E.; Boyle, D.B.; Ramsay, A.J.; Ramshaw, I.A. Evaluation of fowlpox-vaccinia virus prime-boost vaccine strategies for high-level mucosal and systemic immunity against HIV-1. *Vaccine* **2006**, *24*, 5881–5895. [[CrossRef](#)]
64. Wijesundara, D.K.; Xi, Y.; Ranasinghe, C. Unraveling the convoluted biological roles of type I interferons in infection and immunity: A way forward for therapeutics and vaccine design. *Front. Immunol.* **2014**, *5*, 412. [[CrossRef](#)]
65. Rerks-Ngarm, S.; Pitisuttithum, P.; Nitayaphan, S.; Kaewkungwal, J.; Chiu, J.; Paris, R.; Prensri, N.; Namwat, C.; de Souza, M.; Adams, E.; et al. Vaccination with ALVAC and AIDSVAX to Prevent HIV-1 Infection in Thailand. *N. Engl. J. Med.* **2009**, *361*, 2209–2220. [[CrossRef](#)]